
# CCL2/MCP-1 signaling drives extracellular matrix turnover by diverse macrophage subsets

**Henrik J. Jürgensen**[a,b], **Lakmali M. Silva**[a,c], **Oliver Krigslund**[a,b], **Sander van Putten**[b], **Daniel H. Madsen**[b,d,e], **Niels Behrendt**[b], **Lars H. Engelholm**[b] and **Thomas H. Bugge**[a]

***a* - Proteases and Tissue Remodeling Section,** *Oral and Pharyngeal Cancer Branch, National Institute of Dental and Craniofacial Research, National Institutes of Health, 30 Convent Drive, Bethesda, MD 20892, USA*
***b* - Finsen Laboratory,** *Rigshospitalet/BRIC, University of Copenhagen, Ole Maaloesvej 5, DK-2200 Copenhagen N, Denmark*
***c* - Oral Inflammation and Immunity Unit,** *National Institute of Dental and Craniofacial Research, National Institutes of Health, 30 Convent Drive, Bethesda, MD 20892, USA*
***d* - Center for Cancer Immune Therapy (CCIT),** *Department of Haematology, Herlev Hospital, Herlev Ringvej 75, DK-2730 Herlev, Denmark*
***e* - Department of Oncology,** *Herlev Hospital, Herlev Ringvej 75, DK-2730 Herlev, Denmark*

***Correspondence to Thomas H. Bugge:****at: Proteases and Tissue Remodeling Section, Oral and Pharyngeal Cancer Branch, National Institute of Dental and Craniofacial Research, National Institutes of Health, 30 Convent Drive, Room 211, Bethesda, MD 20892, USA. thomas.bugge@nih.gov.*
https://doi.org/10.1016/j.mbplus.2019.03.002
***Thomas H. Bugge:*** *at: Proteases and Tissue Remodeling Section, Oral and Pharyngeal Cancer Branch, National Institute of Dental and Craniofacial Research, National Institutes of Health, 30 Convent Drive, Room 211, Bethesda, MD 20892, USA. thomas.bugge@nih.gov.*
https://doi.org/10.1016/j.mbplus.2019.03.002

## Abstract

Macrophage plasticity, cellular origin, and phenotypic heterogeneity are perpetual challenges for studies addressing the biology of this pivotal immune cell in development, homeostasis, and tissue remodeling/repair. Consequently, a myriad of macrophage subtypes has been described in these contexts. To facilitate the identification of functional macrophage subtypes *in vivo*, here we used a flow cytometry-based assay that allows for detailed phenotyping of macrophages engaged in extracellular matrix (ECM) degradation. Of the five macrophage subtypes identified in the remodeling dermis by using this assay, collagen degradation was primarily executed by $Ly6C^{-}CCR2^{+}$ and $Ly6C^{-}CCR2^{low}$ macrophages *via* mannose receptor-dependent collagen endocytosis, while $Ly6C^{+}CCR2^{+}$ macrophages were the dominant fibrin-endocytosing cells. Unexpectedly, the CCL2/MCP1-CCR2 signaling axis was critical for both collagen and fibrin degradation, while collagen degradation was independent of IL-4Ra signaling. Furthermore, the cytokine GM-CSF selectively enhanced collagen degradation by $Ly6C^{+}CCR2^{+}$ macrophages. This study reveals distinct subsets of macrophages engaged in ECM turnover and identifies novel wound healing-associated functions for CCL2 and GM-CSF inflammatory cytokines.



## Introduction

Postnatal tissue remodeling and tissue regeneration require the orchestrated deposition and removal of extracellular matrix (ECM) proteins within the pericellular environment. Perturbations in ECM homeostasis, due to inadequate or excessive synthesis or degradation of specific ECM components, may cause delayed or aberrant tissue regeneration and, importantly, is linked to the

genesis or progression of a wide variety of common degenerative and inflammatory diseases [1–4]. Two key ECM constituents in this regard are the interstitial collagens, which are deposited by fibroblasts [5,6], and the provisional ECM protein, fibrin, which is formed by the local polymerization and crosslinking of the soluble precursor, fibrinogen [7].

Using intravital microscopy, we have previously developed an assay that allows for the direct visualization of the degradation of fluorescence-labeled ECM components introduced to the mouse dermis [8,9]. Using this assay, we identified a critical role of macrophages in the turnover of both interstitial collagen and fibrin. Furthermore, we found that macrophages execute this catabolic function in a two-step process that involves the initial fragmentation of the ECM by pericellular/extracellular proteases, which is followed by the endocytosis and complete degradation of the fragmented ECM by lysosomal cathepsins. These studies also identified the mannose receptor (MR) and the urokinase plasminogen activator receptor-associated protein (uPARAP) as principal macrophage endocytosis receptors.

The use of intravital microscopy allowed for the identification of specific cell types involved in ECM turnover when combined with *in situ* immunostaining or by using mice with genetically-encoded cell type-specific fluorescent proteins [8,9]. However, this type of assay has restrictions in terms of cellular resolution and throughput, owing to the limited number of cell type-specific markers that can be assessed simultaneously and to the time-consuming nature of quantitative three-dimensional image analysis.

Here we report the development of a flow cytometry-based assay that allows for the detailed phenotyping of macrophage subpopulations engaged in dermal ECM turnover. By using this assay, we show that at least five distinct subpopulations of macrophages are present in the mouse dermis during ECM remodeling. Within these, the dominant macrophage subpopulations engaged in collagen turnover are Ly6C-negative and C-C chemokine receptor type 2 (CCR2) high-expressing cells, and Ly6C-negative CCR2 low-expressing cells, while Ly6C-positive and CCR2-positive macrophages account for the large majority of fibrin-degrading cells. Surprisingly, not only fibrin degradation, but also collagen degradation was dependent on the integrity of the chemokine (C-C motif) ligand 2 (CCL2)/monocyte chemoattractant protein 1 (MCP1)-CCR2 axis. Moreover, macrophage-mediated endocytic collagen degradation was stimulated by Granulocyte Macrophage-Colony Stimulating Factor (GM-CSF), and Interleukin (IL)-13, while IL4-Ra-dependent signaling was dispensable for this process.

## Results

### Identification of matrix-degrading macrophage subtypes by flow cytometry

To set up a flow cytometry-based assay designed to phenotype dermal macrophages engaged in ECM degradation, type-1 collagen was first labeled *ex vivo* with an Alexa Fluor (AF) 647 fluorophore and introduced into mouse dermis by subcutaneous injection as described previously [9]. This procedure leads to the direct association of the injected collagen with preexisting collagen fibers [9]. 24 h after injection of the exogenous fluorescent collagen, the skin surrounding the injection site was resected and placed in a collagenase-containing enzyme mixture to dissociate the dermis and to remove any cell surface-associated fluorescent collagen. The cellular composition of the dermis and the composition of cells associated with the remaining fluorescent collagen, now predominantly in an intracellular form, were then analyzed by flow cytometry. We first tested that our assay could detect macrophages as a dominant cell type in collagen endocytosis and degradation by quantifying the number of macrophages ($CD45^+F4/80^+$ cells), other leukocytes ($CD45^+F4/80^-$ cells) and non-leukocytes ($CD45^-$ cells) associated with the fluorescent collagen (Fig. 1A; Fluorescence minus one controls (FMOs) for the fluorescent collagen are shown in Fig. S1A). This analysis demonstrated that macrophages, other leukocytes, and non-leukocytes constituted 52%, 5%, and 43% of all the detected collagen-endocytosing cells, respectively (Fig. 1B).

We next proceeded to investigate the overall composition of macrophages present in the dermis after injection and to determine whether these were mainly resident macrophages or macrophages recruited as a result of the injection procedure. To do this, all macrophages ($CD45^+F4/80^+$ cells) acquired from dermis with or without injection of exogenous collagen were separated into subpopulations based on no, low or high expression of Ly6C to distinguish resident dermal macrophages (no or low Ly6C expression, designated $Ly6C^-$) and freshly recruited macrophages derived from classical circulating monocytes (high Ly6C expression, designated $Ly6C^+$) [10–12] (Fig. 1C; FMO control for Ly6C is shown in Fig. S1B). Whereas the number of $Ly6C^-$ macrophages did not change upon collagen injection (Fig. 1D), an approximately 8-fold increase in the number of $Ly6C^+$ macrophages was recorded after injection (Fig. 1E), suggesting a substantial recruitment of monocyte-derived macrophages to the injection site. However, even after injection, $Ly6C^-$ resident macrophages remained the most abundant group of macrophages (48% of all cells *vs.* 8% for $Ly6C^+$ macrophages, compare Fig. 1D and E). To

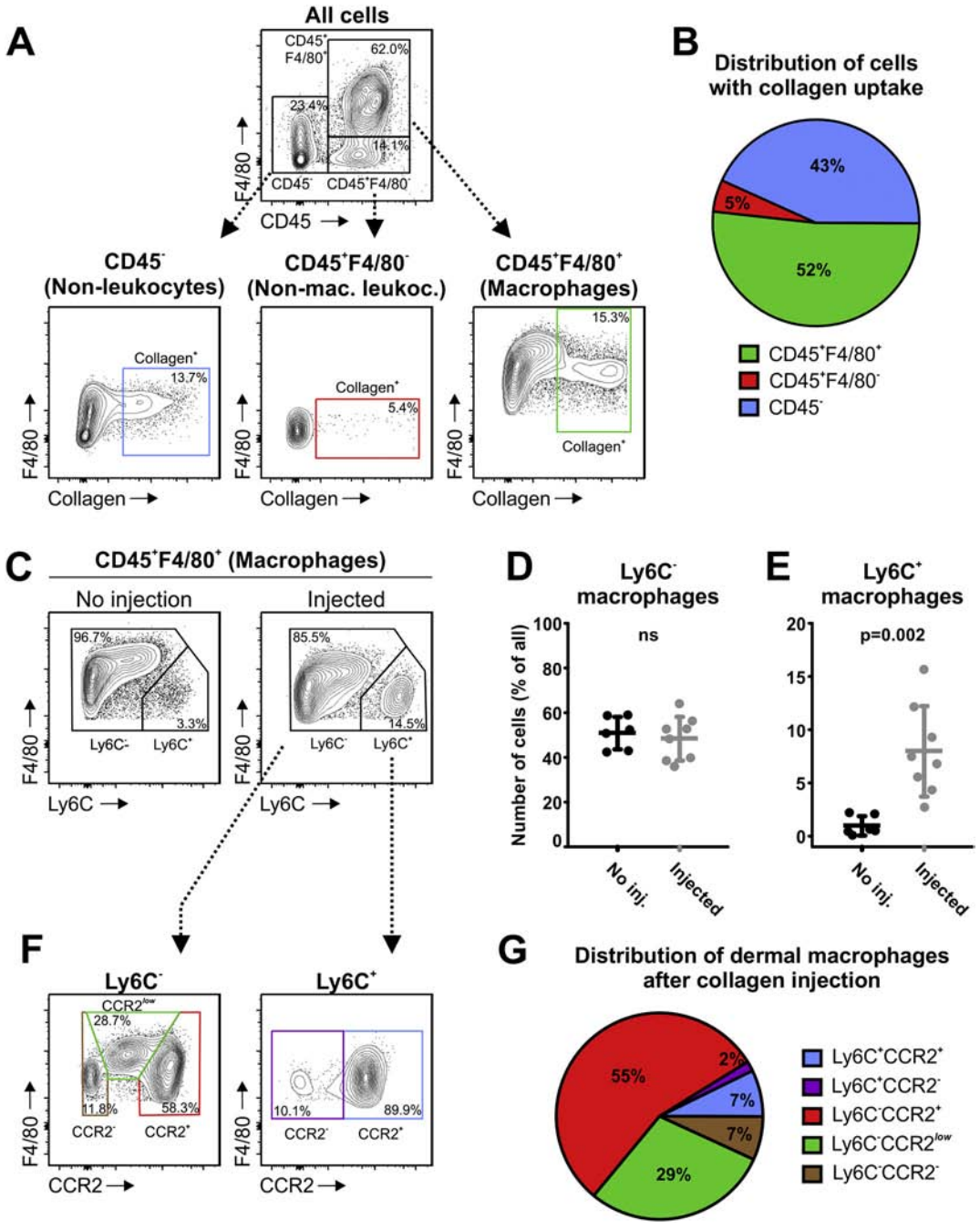


**Fig. 1.** Identification of matrix-endocytosing cells and dermal macrophage subpopulations. (A) Identification of dermal cells engaged in endocytosis and intracellular degradation of AF647-conjugated collagen injected into the dermis. (A, top panel) Separation of dermal cells into macrophages ($CD45^+F4/80^+$ cells), other leukocytes ($CD45^+F4/80^-$ cells) and non-leukocytes ($CD45^-$ cells) by using flow cytometry. (A, bottom panels) Analysis of collagen endocytosis by macrophages, other leukocytes, and non-leukocytes. (B) Pie chart showing the distribution of cells engaged in collagen degradation. (C) Separation of all macrophages ($CD45^+F4/80^+$ cells), acquired from dermis of mice without (left panel) or with (right panel) injection of fluorescent collagen, into a Ly6C-expressing ($Ly6C^+$), recruited subpopulation and a Ly6C non-expressing ($Ly6C^-$), resident subpopulation. (D and E) Quantification of $Ly6C^-$ (D) and $Ly6C^+$ (E) macrophage populations shown in (C), n = 7 (A–E). A two-tailed Student's *t*-test was used to determine significance (D and E). (F) Separation of $Ly6C^-$ (left panel) and $Ly6C^+$ (right panel) macrophages from dermis of mice with injection of fluorescent collagen on the basis of CCR2 expression. $Ly6C^-$ macrophages separated into three distinct populations: $Ly6C^-CCR2^-$, $Ly6C^-CCR2^{low}$, and $Ly6C^-CCR2^+$. $Ly6C^+$ macrophages separated into two distinct populations: $Ly6C^+CCR2^-$ and $Ly6C^+CCR2^+$. (G) Pie chart showing distribution of dermal macrophages shown in (F), n = 5 (F and G).

further investigate the identity of the dermal macrophages, we utilized a knock-in mouse line in which the red fluorescent protein (RFP) gene was inserted into the coding regions of the C-C chemokine Receptor-2 (*Ccr2*) gene, a chemokine receptor expressed by inflammatory macrophages [13]. Analyzing RFP expression in dermal cells from heterozygous mice of this mouse line (carrying one functional allele of the *Ccr2* gene and one allele with RFP expressed under the *Ccr2* promoter, in place of the *Ccr2* gene), allowed for the distinction of $CCR2^+$, inflammatory macrophages, and non-inflammatory macrophages within both the $Ly6C^-$, resident and the $Ly6C^+$, monocyte-derived macrophages (Fig. 1F). Using this approach, five distinct macrophage subtypes were identified, demonstrating the high-resolution potential of this assay, while at the same time illustrating the complexity associated with characterizing subpopulations of macrophages in tissues (Fig. 1F and G, FMO control for RFP is shown in Fig. S1C). $Ly6C^-CCR2^+$ inflammatory macrophages were the most abundant population (constituting 55% of all macrophages) followed by $Ly6C^-CCR2^{low}$ (29%), $Ly6C^+CCR2^+$ (7%) and $Ly6C^-CCR2^-$ (7%) macrophages. $Ly6C^+CCR2^-$ macrophages made up only 2% of the total pool of macrophages and this fraction size was close to the assay's detection limit.

We next quantified the contribution of the five macrophage subtypes identified above to collagen endocytosis and degradation. To do this, all macrophages with a positive association with fluorescent collagen (Fig. 1A, $CD45^+F4/80^+Collagen^+$) were separated on the basis of Ly6C and CCR2 expression (Fig. 2A). This analysis revealed that $Ly6C^-CCR2^+$, $Ly6C^-CCR2^{low}$, and $Ly6C^+CCR2^+$ macrophages all contributed to collagen endocytosis, making up 53%, 30%, and 14% of collagen-endocytosing macrophages (CEMS), respectively (Fig. 2B). The remaining two subtypes of macrophages identified in the dermis made up only a combined 3% of CEMS (Fig. 2B, other macrophages) and were not analyzed further. We also analyzed the amount of endocytosed collagen and found that $Ly6C^-CCR2^+$ macrophages dominated with approximately two and four times more collagen endocytosed, when compared to $Ly6C^-CCR2^{low}$ and $Ly6C^+CCR2^+$ macrophages, respectively (Fig. 2C).

To further characterize the CEMS with respect to surface marker expression, we investigated the expression of CD11b and determined the relative level of F4/80 expression by $Ly6C^-CCR2^+$, $Ly6C^-CCR2^{low}$, and $Ly6C^+CCR2^+$ macrophages. This analysis revealed that the two $Ly6C^-$ macrophage populations expressed the most CD11b, but generally that all of the tested macrophages expressed high levels of this myeloid marker (Fig. S1D). For F4/80, this analysis revealed that the $Ly6C^-CCR2^{low}$ macrophages expressed twice the level of this surface marker, when compared to the two other macrophage populations and, resultantly, could be classified as $F4/80^{High}$ (Fig. S1E).

Due to the surprisingly large contribution of CCR2-positive inflammatory macrophages to collagen degradation (a combined 67% of all CEMS expressed CCR2, Fig. 2B), a process otherwise reported to be dominated by macrophages with a non-inflammatory, wound-healing phenotype [14], we investigated the role of the CCL2/MCP1-CCR2 signaling axis in the macrophage-mediated endocytosis of collagen. To do this, we compared the macrophage presence after injection of fluorescent collagen into the dermis of CCR2.RFP heterozygous (*Ccr2* +/–) and CCR2.RFP homozygous (*Ccr2* –/–) mice. This investigation revealed a modest reduction (29%) in the total number of macrophages, due to the loss of CCR2 (Fig. 2D), but a much larger reduction (50%) in the number of CEMS (Fig. 2E). This reduction was the result of a loss of CEMS belonging to both the resident $Ly6C^-$ (Fig. 2F) and the recruited $Ly6C^+$ (Fig. 2G) populations. Consequently, macrophage-associated collagen endocytosis is highly dependent on CCR2-mediated signaling, both with respect to the recruitment of inflammatory $Ly6C^+$ macrophages, and with respect to $Ly6C^-$ inflammatory macrophages already in place in the dermis before tissue insult.

An overview of the properties ascribed to each subpopulation of CEMS thus far, including surface marker expression and status as recruited or resident macrophage type, is summarized in Table 1.

## Dextran uptake distinguishes inflammatory and wound healing resident macrophages engaged in collagen degradation in dermis

To further explore the identities and phenotypes of collagen-degrading inflammatory ($Ly6C^+CCR2^+$ and $Ly6C^-CCR2^+$) and non-inflammatory macrophages ($Ly6C^-CCR2^{low}$), we combined collagen injection with the injection of 10 kDa fluorescent dextran, a compound preferentially taken up by macrophages with a wound-healing, M2-like phenotype [9,15,16]. When analyzing the dextran uptake by $Ly6C^-$ CEMS, we were able to separate these into populations with a low and high uptake of dextran (Fig. 3A, top left panel). In contrast, the $Ly6C^+$ CEMS all had a low dextran uptake (Fig. 3A, top right panel), consistent with nearly all of these being inflammatory $CCR2^+$ macrophages (Fig. 2A, right panel). We then separated the $Ly6C^-$ CEMS with a low and high dextran uptake on the basis of CCR2 expression (Fig. 3A, lower panels), and found that nearly all $Ly6C^-Dex^{low}$ CEMS belonged to the $CCR2^+$ population (Fig. 3B) and the large majority of $Ly6C^-Dex^{high}$ CEMS belonged to the $CCR2^{low}$ population (Fig. 3C). In a control experiment, we

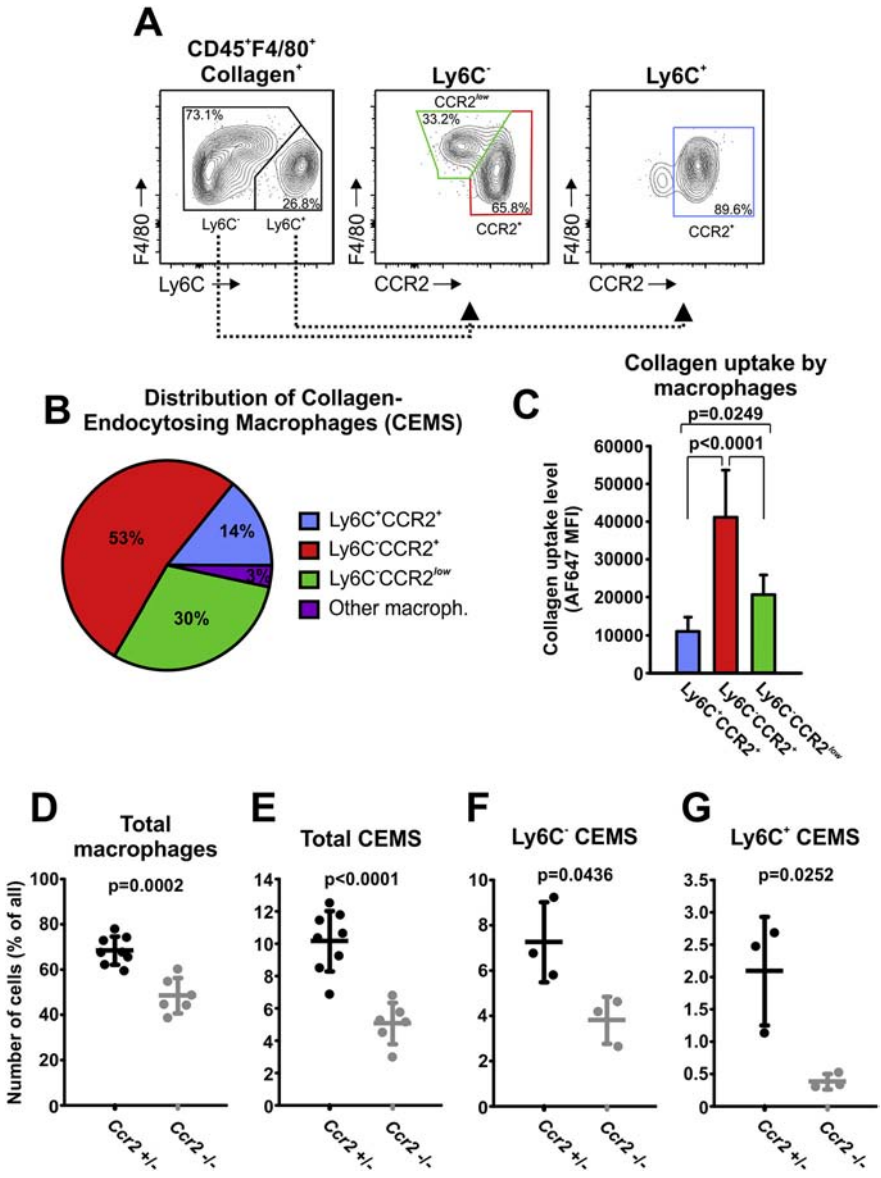


**Fig. 2.** Deletion of CCR2 attenuates macrophage-mediated collagen degradation in mouse dermis. (A–C) Inflammatory macrophages dominate collagen degradation. (A) Separation of macrophages positive for endocytosis of fluorescent collagen ($CD45^+F4/80^+Collagen^+$ cells) into subpopulations on the basis of Ly6C expression (left panel). Separation of $Ly6C^-$ and $Ly6C^+$ populations on the basis of CCR2 expression (center and right panels, respectively). This analysis revealed three principal subpopulations of CEMS: $Ly6C^-CCR2^+$, $Ly6C^-CCR2^{low}$, and $Ly6C^+CCR2^+$ cells. (B) Pie chart showing the distribution of CEMS shown in (A). (C) Quantification of collagen uptake level in subpopulations of CEMS shown in (A), n = 5 (A–C). (D–G) CCR2 is critical for macrophage-associated collagen degradation. Quantification of all macrophages (D), all CEMS (E), $Ly6C^-$ CEMS (F), and $Ly6C^+$ CEMS (G) in dermis of CCR2-deficient mice (*Ccr2* –/–) and CCR2-expressing littermates (*Ccr2* +/–) with injection of fluorescent collagen, n = 6–8 (D and E), n = 3 (F and G). A two-tailed Student's *t*-test was used to determine significance.

also performed separation of the macrophage subpopulations in the reverse order, *i.e.*, we first separated CEMS into $Ly6C^-CCR2^+$, $Ly6C^-CCR2^{low}$, and $Ly6C^+CCR2^+$ subpopulations and then quantified the dextran uptake by each of these (Fig. 3D). This experiment confirmed the very high dextran uptake by $Ly6C^-CCR2^{low}$ CEMS, consistent with a wound healing, M2-like phenotype, and low dextran uptake by both $Ly6C^-CCR2^+$ and $Ly6C^+CCR2^+$ CEMS, consistent with an inflammatory, M1-like phenotype. We also examined the role of the CCL2/MCP1-CCR2 signaling axis in collagen endocytosis by subpopulations of macrophages separated on the basis of dextran uptake capability

**Table 1.** Properties of matrix-endocytosing macrophage subtypes. Overview of surface marker expression, status as recruited or resident macrophage type, ECM uptake potential, dextran uptake potential, and endocytic collagen receptor employed for collagen uptake for each of the three principal matrix-degrading macrophage subpopulations described in this study.

| Macrophage subtype | Surface marker expression | ECM uptake potential | Recruited or resident | Dextran uptake | Collagen endocytosis mechanism |
|---|---|---|---|---|---|
| Inflammatory, M1 | $F4/80^+CD11b^+$ $Ly6C^+CCR2^+MR^{low}$ | Collagen: intermediate Fibrin: high | CCR2-dependent recruitment to injured dermis | Low | uPARAP-dependent |
| Inflammatory, M1 | $F4/80^+CD11b^+$ $Ly6C^-CCR2^+MR^{int}$ | Collagen: high Fibrin: intermediate | CCR2-dependent recruitment to normal dermis | Low | MR-dependent |
| Wound-healing, M2 | $F4/80^+CD11b^+$ $Ly6C^-CCR2^{low}MR^{High}$ | Collagen: high Fibrin: low | Resident dermal macrophage | High | MR-dependent |

(Fig. 3E and F). In accordance with the high expression of CCR2 by the $dex^{low}$ macrophages, this analysis revealed that the number of $Dex^{low}$ CEMS (including both $Ly6C^+Dex^{low}$ and $Ly6C^-Dex^{low}$ macrophages, see Fig. 3A) was reduced by nearly 75% in the *Ccr2* –/– mice (Fig. 3E). In contrast, the $Dex^{high}$ CEMS were unaffected by the loss of CCR2 (Fig. 3F), which was in accordance with the low expression of CCR2 by these cells. Altogether, these experiments demonstrate that

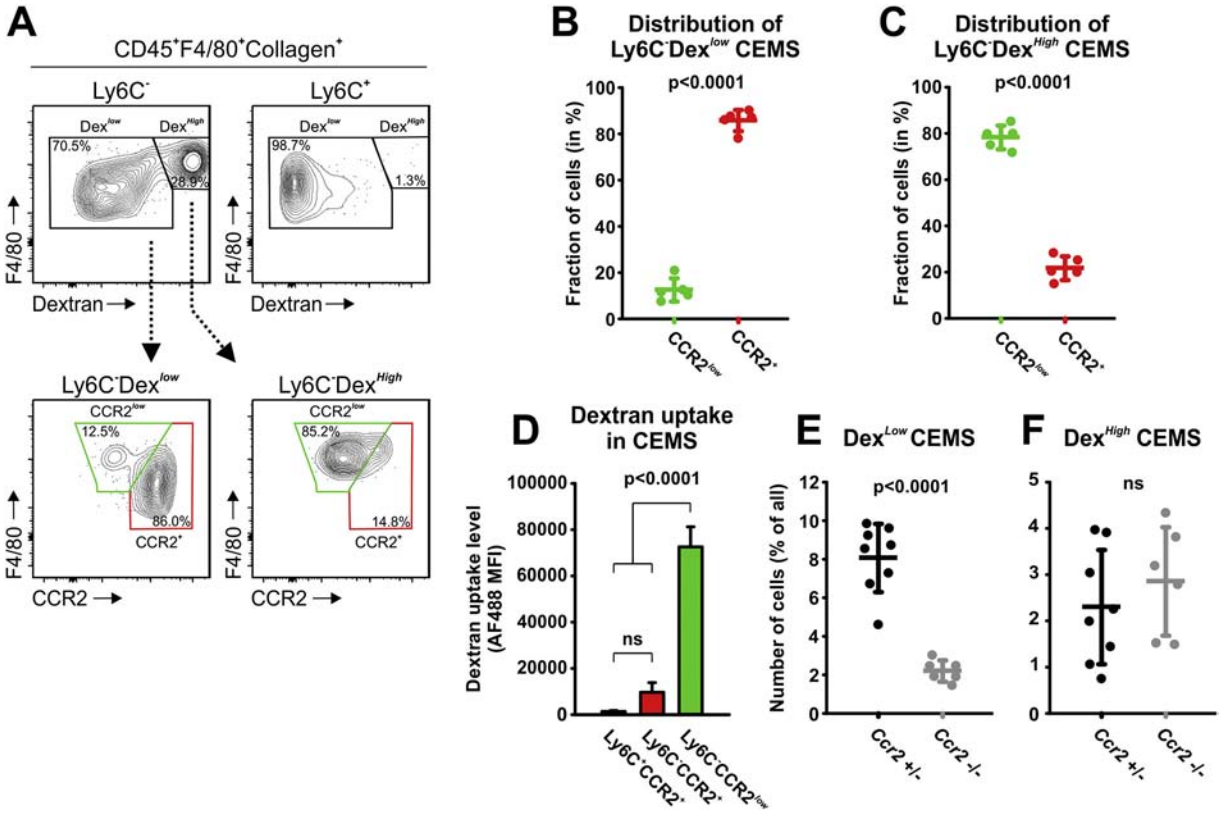


**Fig. 3.** A high capacity for dextran uptake distinguishes collagen-degrading $Ly6C^-CCR2^{low}$ wound-healing macrophages from collagen-degrading $Ly6C^-CCR2^+$ inflammatory macrophages. (A, top) Separation of $Ly6C^-$ (left panel) and $Ly6C^+$ (right panel) CEMS ($CD45^+F4/80^+Collagen^+$) on the basis of their capacity for uptake of AF488-conjugated fluorescent dextran injected into the dermis together with fluorescent collagen (AF647-conjugated). (A, bottom) Separation of $Ly6C^-Dex^{low}$ (left panel) and $Ly6C^-Dex^{high}$ (right panel) CEMS on the basis of CCR2 expression. (B and C) Quantification of $Ly6C^-CCR2^+$ and $Ly6C^-CCR2^{low}$ CEMS within the $Ly6C^-Dex^{low}$ (B) and $Ly6C^-Dex^{high}$ (C) populations. (D) Quantification of dextran uptake level in $Ly6C^+CCR2^+$, $Ly6C^-CCR2^+$, and $Ly6C^-CCR2^{low}$ CEMS, n = 5 (B–D). (E and F) Quantification of $Dex^{low}$ (E) and $Dex^{high}$ (F) CEMS in dermis of CCR2-deficient mice (*Ccr2* –/–) and CCR2-expressing littermates (*Ccr2* +/–) with injection of fluorescent collagen (AF647) and fluorescent dextran (AF488), n = 6–8. Two-tailed Student's *t*-test (B, C, E and F) or one-way ANOVA (D) was used to test for significance.

the combination of dextran uptake potential and Ly6C expression are sufficient parameters to distinguish between Ly6C$^-$CCR2$^+$Dex$^{low}$, Ly6C$^-$CCR2$^{low}$Dex$^{high}$, and Ly6C$^+$CCR2$^+$Dex$^{low}$ CEMS (Dextran uptake potential for each subpopulation is also listed in Table 1).

### Ly6C$^-$ resident dermal macrophages and Ly6C$^+$ recruited macrophages utilize distinct pathways for collagen internalization dependent on either the mannose receptor or uPARAP

The endocytic receptor known as the mannose receptor (MR, CD206) binds and internalizes collagens, and it enables intracellular collagen degradation by macrophages in various *in vitro* and *in vivo* assays [9,17–19]. However, these previously employed assays did not allow for evaluation of the contribution of MR to collagen endocytosis by individual macrophage subtypes *in vivo*. We therefore utilized our flow cytometry-based assay to evaluate the importance of MR in collagen-endocytosis by distinct macrophage subpopulations. We initially analyzed each identified subpopulation of CEMS for the expression of MR (Fig. 4A and B). This analysis revealed a large difference in the level of MR expression, with a very high expression recorded in the Ly6C$^-$CCR2$^{low}$Dex$^{high}$ population, an intermediate expression in the Ly6C$^-$CCR2$^+$Dex$^{low}$ population, and a low expression in the Ly6C$^+$CCR2$^+$Dex$^{low}$ population. A separate control experiment in which the fluorescent signal recorded from all F4/80$^+$ dermal macrophages isolated from wild type (*Mrc1* +/+) or MR-deficient (*Mrc1* –/–) mice stained with the anti-MR antibody confirmed that the MR stain was specific (Fig. 4C). We then investigated collagen-endocytosis in the dermal macrophages isolated from MR-deficient mice and littermate wild type controls. CEMS were again separated into Ly6C$^-$ and Ly6C$^+$ populations, but when attempting to separate Ly6C$^-$ CEMS based on fluorescent dextran uptake as described in Fig. 3, it became apparent that a profound contribution of MR to the uptake of this bacterial polysaccharide entity (Fig. S2), a function of MR also reported to enable dextran uptake by dendritic cells [20], prohibited the further separation of Ly6C$^-$ CEMS into Ly6C$^-$CCR2$^+$Dex$^{low}$ and Ly6C$^-$CCR2$^{low}$Dex$^{high}$ in these mice. As a result, we investigated the role of MR in collagen endocytosis in resident (both Ly6C$^-$CCR2$^+$ and Ly6C$^-$CCR2$^{low}$) and recruited (Ly6C$^+$CCR2$^+$) macrophages separated on the basis of Ly6C expression only (Fig. 4D). In this experiment, a large reduction in collagen endocytosis was noted for the MR-deficient Ly6C$^-$ macrophages (Fig. 4E, left panel). In contrast, collagen endocytosis by Ly6C$^+$ macrophages was not affected by the loss of MR (Fig. 4F, left panel). To explore other possible mechanisms involved in collagen endocytosis by Ly6C$^+$ macrophages, we then focused on uPARAP (Endo180, CD280), an MR-related endocytic receptor known to facilitate collagen uptake mainly by cells of mesenchymal origin, but also with additional minor contributions in macrophages [9,21–23]. When examining macrophages from uPARAP-deficient mice (*Mrc2* –/–) and littermate controls (*Mrc2* +/+), a small, non-significant difference in collagen endocytosis was recorded for the Ly6C$^-$ macrophage population (Fig. 4E, right panel), suggesting that these macrophages depend mainly on MR in this process. However, a reduction in collagen endocytosis by the Ly6C$^+$ macrophages was indeed observed in the uPARAP-deficient mice (Fig. 4F, right panel). The endocytic collagen receptor utilized for collagen uptake by each macrophage subpopulation is also listed in Table 1.

To further pursue the differential dependence on MR or uPARAP for collagen endocytosis by subtypes of macrophages, we performed *in vitro* differentiation of mouse bone marrow cells into macrophages using different combinations of stimulatory cytokines (M-CSF, GM-CSF, IL-4 and IL-13). We first analyzed the expression of MR and uPARAP by the bone marrow-derived macrophages using Western blotting (Fig. 4G). MR expression was generally high in M-CSF macrophages and was further increased by both IL-4 and IL-13. M-CSF macrophages also expressed uPARAP, but this was, in contrast to MR, reduced by the addition of IL-4. GM-CSF-stimulated bone marrow cells expressed very low levels of the two receptors under the tested conditions. The specificity of the signal obtained when using primary anti-MR and anti-uPARAP antibodies in the Western blot analysis was verified by including M-CSF- and IL-13-stimulated macrophages from MR-deficient and uPARAP-deficient mice (Fig. 4H). We also performed a functional test of the contribution of MR and uPARAP to collagen endocytosis by bone marrow-derived macrophages differentiated using M-CSF. In all macrophages tested, the endocytosis of fluorescent collagen added in solution was almost completely abrogated in macrophages from MR-deficient mice (Fig. 4I), in line with the high MR expression by these cells. Loss of uPARAP, however, only produced a marginal reduction in collagen endocytosis by the macrophages with the highest uPARAP expression (M-CSF alone or M-CSF + IL-13, Fig. 4J). Altogether, the *in vitro* experiment demonstrated that macrophages can be stimulated to express both MR and uPARAP, but that collagen endocytosis mainly depends on MR in highly differentiated bone marrow-derived macrophages.

### GM-CSF and IL-13 promote collagen degradation by Ly6C$^+$CCR2$^+$ macrophages

Spurred by the dominant role of inflammatory macrophages in the endocytosis and degradation of collagen, we wanted to investigate how a variety of

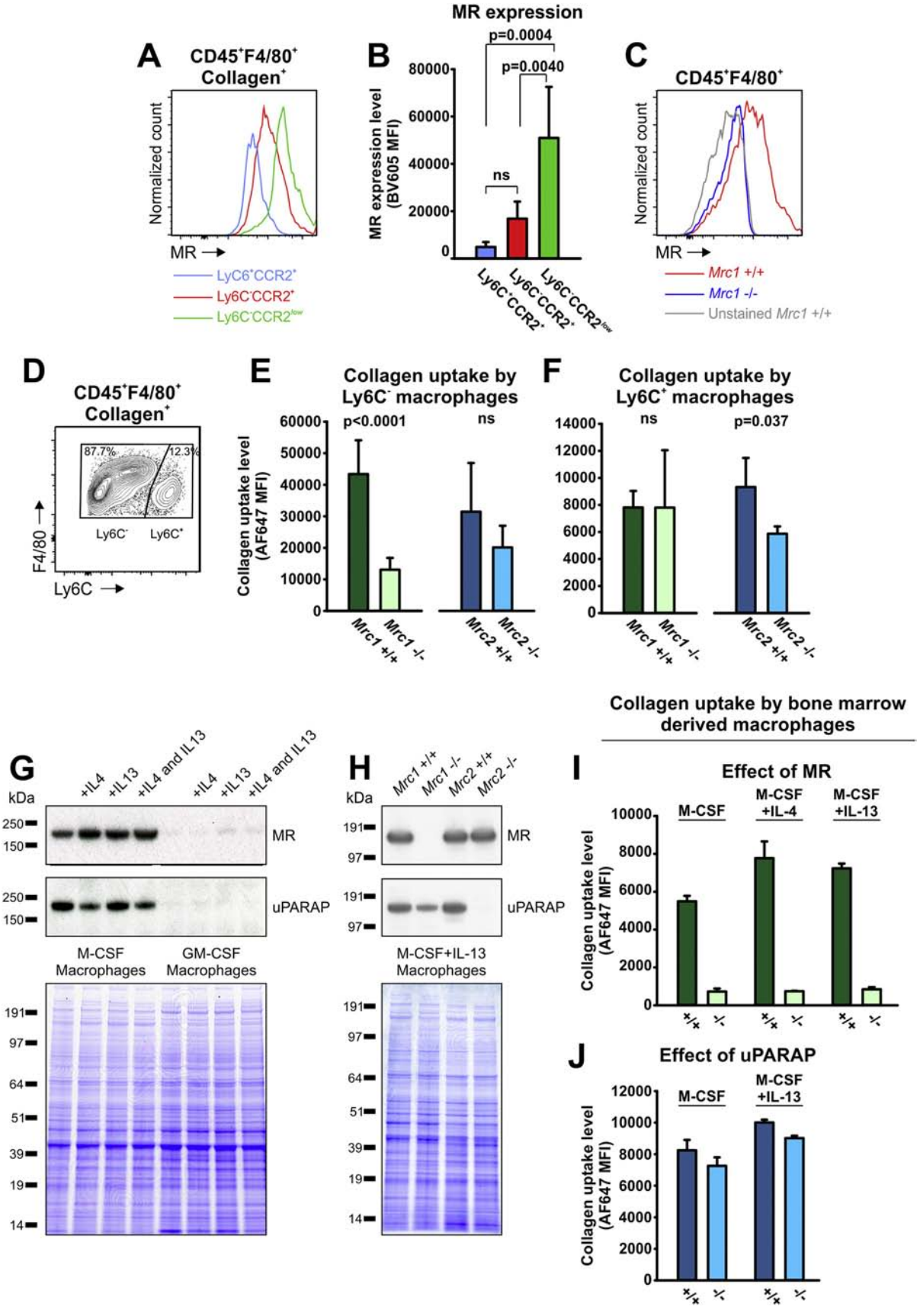
A
CD45+F4/80+ Collagen+
Normalized count
MR
LyC6+CCR2+
Ly6C-CCR2+
Ly6C-CCR2low
B
MR expression
p=0.0004
p=0.0040
ns
MR expression level (BV605 MFI)
Ly6C+CCR2+
Ly6C-CCR2+
Ly6C-CCR2low
C
CD45+F4/80+
Normalized count
MR
Mrc1 +/+
Mrc1 -/-
Unstained Mrc1 +/+
D
CD45+F4/80+ Collagen+
87.7%
12.3%
Ly6C-
Ly6C+
F4/80
Ly6C
E
Collagen uptake by Ly6C- macrophages
p<0.0001
ns
Collagen uptake level (AF647 MFI)
Mrc1 +/+
Mrc1 -/-
Mrc2 +/+
Mrc2 -/-
F
Collagen uptake by Ly6C+ macrophages
ns
p=0.037
Mrc1 +/+
Mrc1 -/-
Mrc2 +/+
Mrc2 -/-
G
kDa
+IL4
+IL13
+IL4 and IL13
+IL4
+IL13
+IL4 and IL13
MR
uPARAP
M-CSF Macrophages
GM-CSF Macrophages
H
kDa
Mrc1 +/+
Mrc1 -/-
Mrc2 +/+
Mrc2 -/-
MR
uPARAP
M-CSF+IL-13 Macrophages
Collagen uptake by bone marrow derived macrophages
I
Effect of MR
M-CSF
M-CSF +IL-4
M-CSF +IL-13
Collagen uptake level (AF647 MFI)
+/+
-/-
J
Effect of uPARAP
M-CSF
M-CSF +IL-13
Collagen uptake level (AF647 MFI)
+/+
-/-

macrophage-stimulatory cytokines effected the activity of different macrophages *in vivo*. Therefore, the pleiotropic GM-CSF [24–26] or each of the wound healing-associated cytokines M-CSF, IL-4 and IL-13 [27–32] was included in the fluorescent collagen before subcutaneous injection. 24 h after injection, each subtype of CEMS (Fig. 5A) were quantified and compared to controls in which no cytokine had been included. Ly6C$^+$CCR2$^+$ recruited macrophages responded vigorously to both GM-CSF and IL-13, with a, respectively, 3.6-fold and 2.9-fold increase in the number of CEMS of this subtype (Fig. 5B, left panel). In contrast, the cytokines had little or no effect on the Ly6C$^-$ macrophage subtypes, with only IL-4 inducing a statistically significant response (1.5-fold increase in the number of Ly6C$^-$CCR2$^+$Dex$^{low}$) (Fig. 5B, center and right panel). We also quantified the amount of collagen endocytosed and the expression of MR by the macrophage subtypes after cytokine injection. However, only marginal effects on these parameters were observed, with the most pronounced positive effect being a 1.7-fold increase in collagen uptake and MR expression by Ly6C$^+$CCR2$^+$ macrophages induced by IL-4 (Fig. S3A and B). To deduce the mechanism behind the effects of GM-CSF and IL-13, we quantified the total number of Ly6C$^+$ and Ly6C$^-$ macrophages in the dermis after cytokine stimulation. This analysis revealed that both cytokines specifically increased the total number of Ly6C$^+$CCR2$^+$ macrophages (2.2 and 1.7-fold increase, respectively) (Fig. 5C, right panel), although the increase caused by IL-13 just failed to reach statistical significance, suggesting a stimulatory effect of the cytokines on recruitment or proliferation of these cells. To test these possibilities further, we examined the effect of GM-CSF on the proliferation of cultured bone marrow cells. In this experiment, GM-CSF caused a large increase in total cell number after 4 days of culture when compared to M-CSF stimulated or unstimulated cells (Fig. 5D). Finally, we also examined the expression of receptors for GM-CSF (GM-CSFR, CD116) and IL-4/IL-13 (IL4Ra, CD124) by the macrophage subtypes *in vivo* using flow cytometry. This analysis revealed that GM-CSFR and IL4Ra were expressed by not only Ly6C$^+$CCR2$^+$ macrophages, but also by the majority of macrophages from the Ly6C$^-$ subtypes (Fig. S4). Taken together, these observations suggest that GM-CSF and IL-13 induce proliferation of Ly6C$^+$CCR2$^+$ macrophages through a direct binding to their receptors on the surface of these cells. However, they offer no explanation as to why these cytokines do not induce proliferation of the Ly6C$^-$ macrophage subpopulations.

In the light of the IL-4 stimulation of MR expression and collagen degradation observed in our experiment with cultured bone marrow macrophages (Fig. 4) and the linkage of IL-4 to a wound-healing macrophage phenotype [32–36], the small effects of this cytokine observed in our *in vivo* collagen degradation model were surprising. This could perhaps be explained by the short time of exposure of cells to the cytokine (24 h) or by the fact that IL-4 already exerted its functions to differentiate resident macrophages, which prohibited further stimulation by exogenous IL-4. To test the latter possibility, we examined the overall role of IL-4 signaling in collagen degradation by injecting fluorescent collagen into the dermis of IL4Ra-deficient mice, in which IL-4- and canonical IL-13-mediated signaling is abolished [37]. However, when comparing IL4Ra-deficient mice to littermate wild type controls, no difference in the number of CEMS of each subtype (Fig. 6A–C, left panels) or the amount of collagen internalized by these cells (Fig. 6A–C, center panels)

**Fig. 4.** Ly6C$^-$ and Ly6C$^+$ macrophages employ distinct receptors for collagen endocytosis. (A–C) Expression of MR by dermal CEMS. (A) Histogram showing an example of MR expression by Ly6C$^+$CCR2$^+$, Ly6C$^-$CCR2$^{low}$, and Ly6C$^-$CCR2$^+$ macrophages analyzed by flow cytometry. (B) Quantification of the MR expression level by macrophage populations shown in A, n = 5. One-way ANOVA was used to test for significance. (C) Control experiment demonstrating specificity of anti-MR antibody used in flow analysis for MR expression shown in A and B. Note that the fluorescent signal from macrophages isolated from *Mrc1* –/– mice stained with the anti-MR antibody is identical to the fluorescent signal acquired from unstained *Mrc1* +/+ macrophages. (D-F) Separation of dermal CEMS into Ly6C$^-$ and Ly6C$^+$ subpopulations after s.c. injection of fluorescent collagen into the dermis and evaluation of the contribution of collagen receptors to collagen endocytosis by each population. (E–F) Quantification of collagen uptake in Ly6C$^-$ (E) and Ly6C$^+$ (F) CEMS from MR-deficient (*Mrc1* –/–, left panels), uPARAP-deficient (Mrc2 –/–, right panels) and the corresponding littermate wild type controls (*Mrc1* +/+ and *Mrc2* +/+, respectively), n = 7 (E–F, left panels), n = 3–5 (E–F, right panels). A two-tailed Student's *t*-test was used to test for significance. (G–J) Expression of endocytic collagen receptors and evaluation of collagen endocytosis by macrophages differentiated from bone marrow cells acquired from MR-deficient (*Mrc1* –/–) and uPARAP-deficient (*Mrc2* –/–) mice and corresponding wild type littermates. (G) Western blot analysis for the expression of MR (top panel) and uPARAP (center panel) by wild type bone-marrow derived macrophages differentiated using M-CSF or GM-CSF alone or in combinations with IL-4 and/or IL-13. The experiment was performed three times with similar results. (H) Verification of anti-MR (top panel) and anti-uPARAP (center panel) primary antibody specificity in Western blot analysis for receptor expression by M-CSF/IL-13 stimulated bone marrow-derived macrophages. Coomassie brilliant blue stains were included as loading controls (G and H, bottom panel). (I and J) Endocytosis of AF647-conjugated collagen by bone marrow-derived macrophages differentiated using M-CSF alone or together with IL-4 or IL-13, n = 2–3.

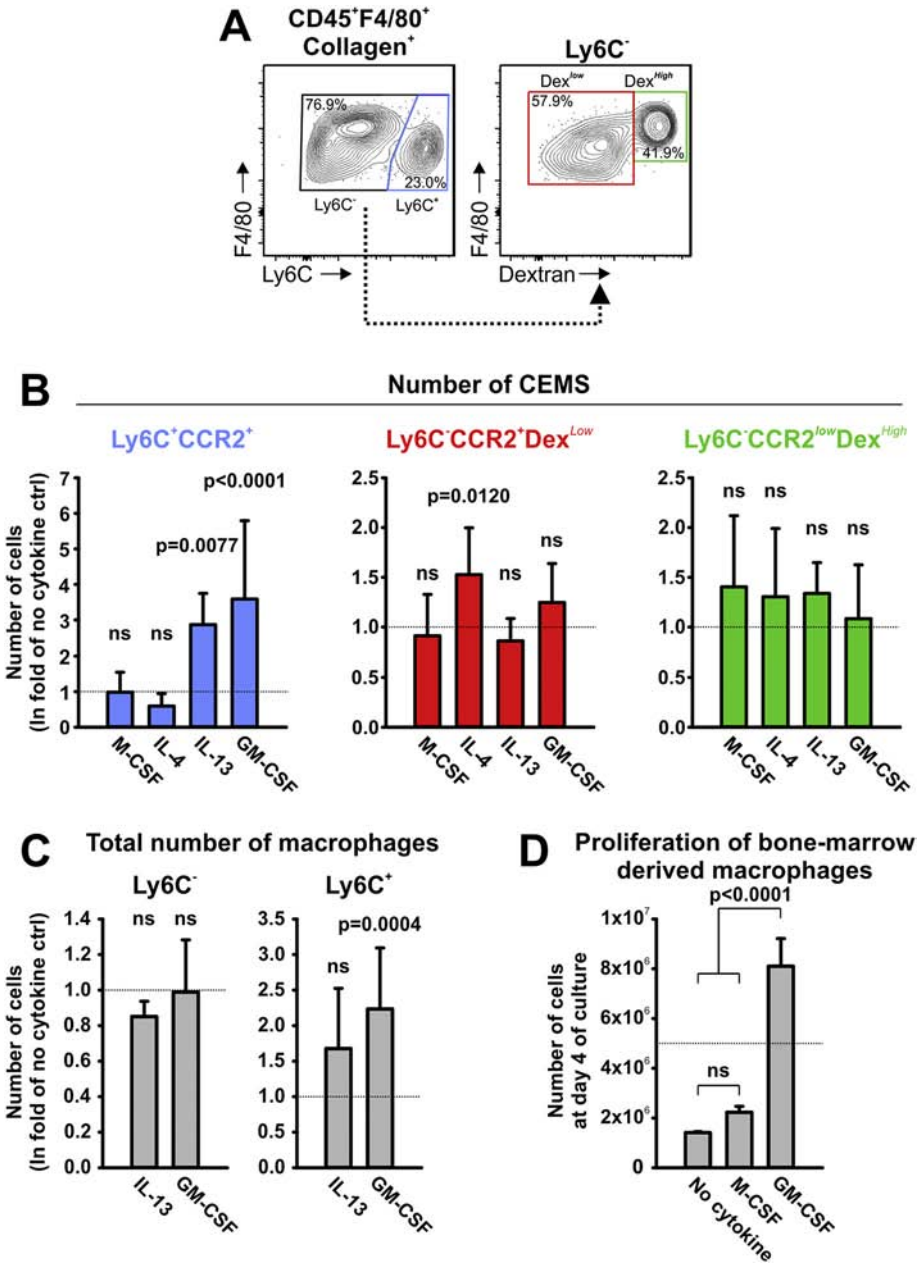


**Fig. 5.** Effect of inflammatory and wound healing-associated cytokines on macrophage-mediated endocytic collagen degradation in dermis. (A and B) Effect of M-CSF, IL-4, IL-13 and GM-CSF on collagen endocytosis by Ly6C$^+$CCR2$^+$ (blue), Ly6C$^-$ CCR2$^+$ Dex$^{low}$ (red), and Ly6C$^-$CCR2$^{low}$Dex$^{High}$ (green) macrophage subpopulations after s.c. injection of fluorescent collagen mixed with each cytokine. The effect of each cytokine is presented as a relative comparison of the number of CEMS to the number obtained using control mice in which cytokine injection was omitted (B). (C) Quantification of the total number of Ly6C$^-$ (left panel) and Ly6C$^+$ (right panel) macrophages following GM-CSF and IL-13 injection into mouse dermis relative to control mice with no cytokine injected, n = 6–8 (B and C). (D) Proliferation of bone marrow-derived macrophages differentiated using M-CSF or GM-CSF. Total cell counts were determined after 4 days of culture in the presence of M-CSF or GM-CSF, or in the absence of cytokine. $5 \times 10^6$ bone marrow cells were seeded for each condition, n = 3–5. A one-way ANOVA was used to test for significance (B–D).

was observed, and only Ly6C$^-$CCR2$^{low}$Dex$^{High}$ macrophages displayed a marginal reduction in MR expression (Fig. 6A–C, right panels). Consequently, IL-4 signaling is dispensable for the recruitment and phenotypes of Ly6C$^+$ macrophages as well as resident Ly6C$^-$ macrophages with respect to endocytic collagen degradation activity *in vivo*.

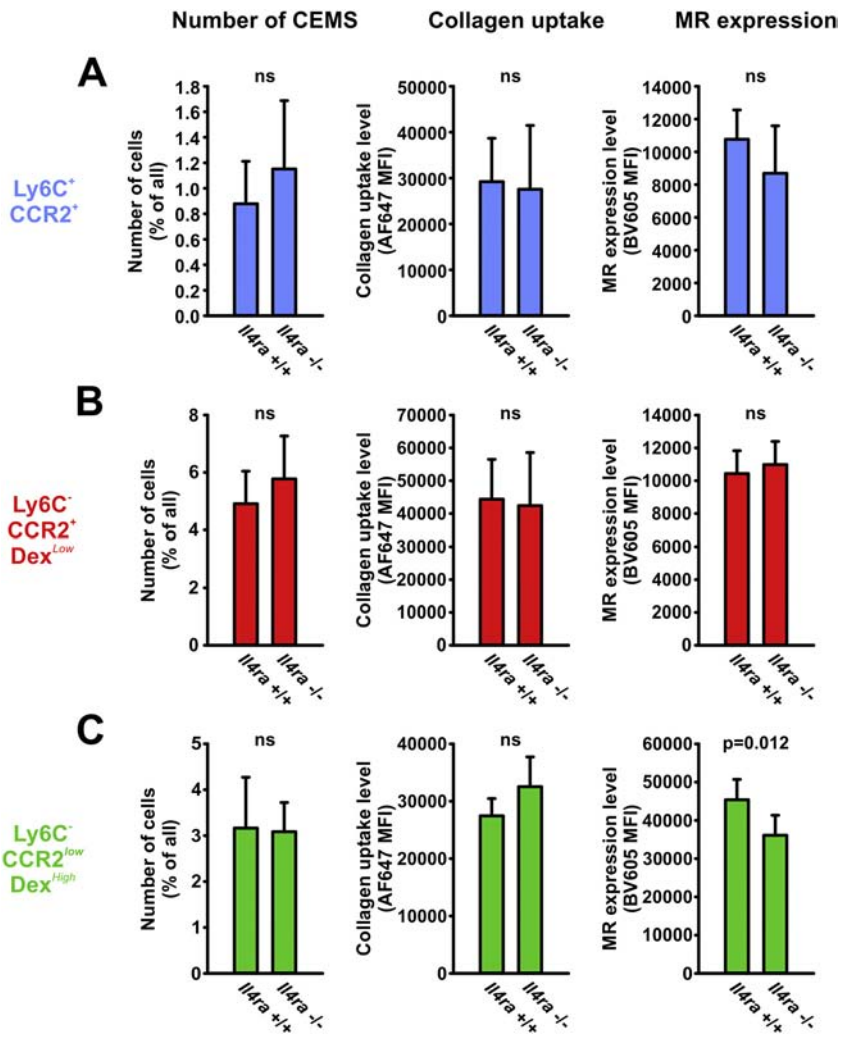


**Fig. 6.** Effect of IL4Ra-signaling on macrophage-mediated endocytic collagen degradation in dermis. (A–C) Evaluation of collagen endocytosis and MR expression by macrophages after injection of fluorescent collagen into dermis of IL4Ra-deficient mice (*Il4ra* –/–) and wild type littermate controls (*Il4ra* +/+). The number of collagen-endocytosing cells (left panels), the amount of collagen endocytosed (center panels) and the expression of MR (right panels) were determined for Ly6C$^{+}$CCR2$^{+}$ (A, blue), Ly6C$^{-}$CCR2$^{+}$Dex$^{low}$ CCR2$^{+}$ (B, red), and Ly6C$^{-}$CCR2$^{low}$Dex$^{High}$ (C, green) macrophage subpopulations, n = 6. A two-tailed Student's *t*-test was used to test for significance.

### CCL2/MCP-1-elicited Ly6C$^{+}$CCR2$^{+}$ inflammatory macrophages dominate fibrin endocytosis and degradation *in vivo*

Using intravital microscopy, we recently identified a novel endocytic pathway for the degradation of extravascular fibrin in lysosomes, undertaken by a population of CCR2$^{+}$ inflammatory macrophages in a plasminogen-dependent process [8]. To take advantage of the flow cytometry-based assay's improved resolution and quantitative potential, as demonstrated in the collagen endocytosis assay above, we also investigated the role of macrophage subtypes involved in fibrin endocytosis and degradation using this approach. Fibrin gels formed *ex vivo* with 1% AF647-labeled fibrin incorporated, were placed in the subcutaneous extravascular space and 24 h later, the dermis covering the implanted fibrin gels was resected and subjected to enzymatic dissociation to generate a single cell suspension. The association of macrophages (CD45$^{+}$F4/80$^{+}$ cells) with the fluorescent fibrin was then analyzed by flow cytometry (Fig. 7A). We first analyzed fibrin uptake in macrophages from the dermis of plasminogen-deficient (*Plg* –/–) mice and wild type littermates (*Plg* +/+) and found that the loss of plasminogen completely abrogated the uptake of fibrin by macrophages (Fig. 7B), effectively recapitulating the results from the intravital microscopy study [8]. We then utilized CCR2.RFP heterozygous

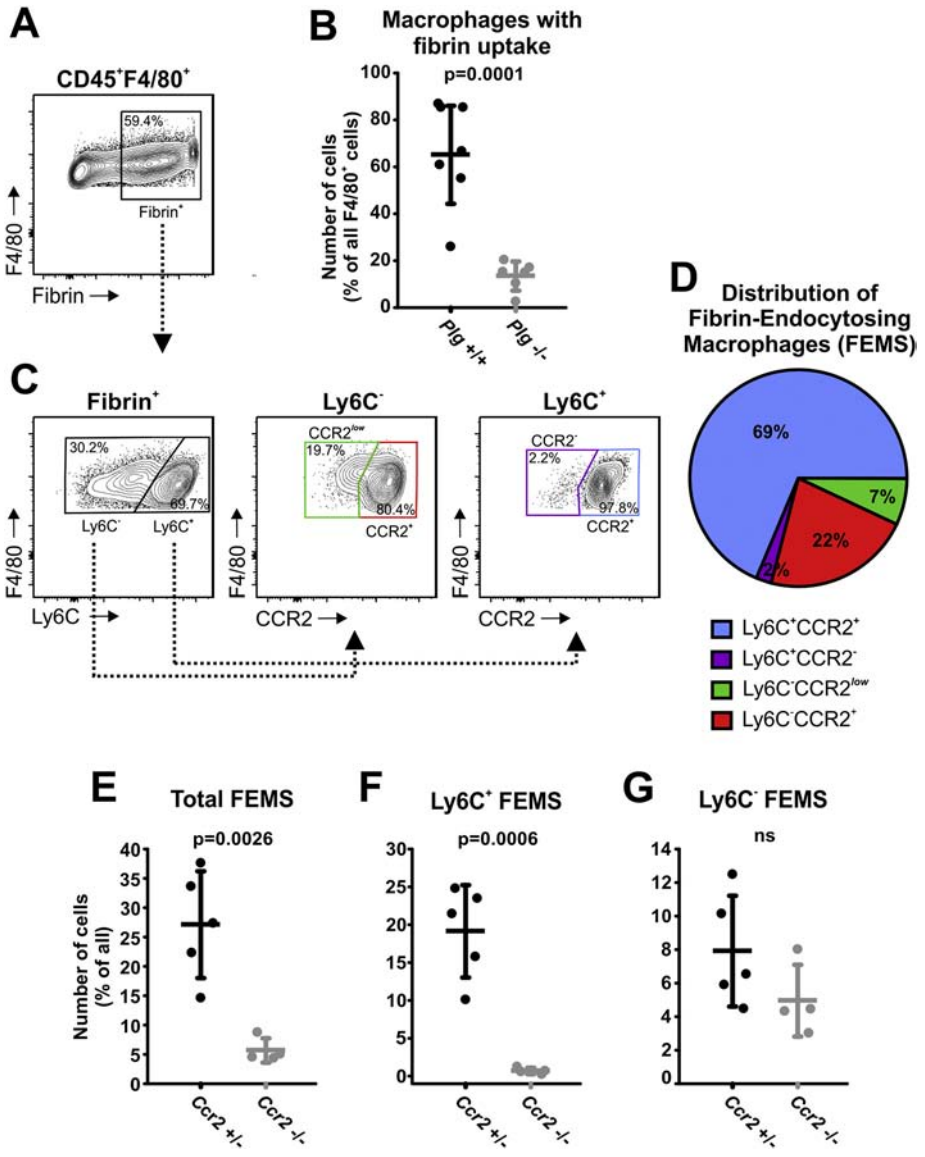


**Fig. 7.** Recruitment of fibrin-degrading inflammatory macrophages depends on CCR2-signaling. (A) Analysis of fibrin-endocytosing macrophages ($CD45^+F4/80^+Fibrin^+$ cells) detected by using flow cytometry following implantation of fibrin gels containing fluorescent AF647-conjugated fibrin into the subcutaneous space. (B) Macrophage-mediated fibrin endocytosis depends on plasminogen. The endocytosis of fibrin by macrophages was evaluated following implantation of fluorescent fibrin gels in plasminogen-deficient mice (*Plg* –/–) and wild type littermates (*Plg* +/+), n = 6–7. (C–D) $Ly6C^+CCR2^+$ inflammatory macrophages are the principal fibrin-endocytosing cells. (C) Separation of FEMS ($Fibrin^+$) on the basis of Ly6C expression (left panel) followed by the separation of $Ly6C^-$ (center panel) and $Ly6C^+$ (right panel) macrophages on the basis of CCR2 expression. Four separate subpopulations of FEMS were identified: $Ly6C^-CCR2^{low}$ (green), $Ly6C^-CCR2^+$ (red), $Ly6C^+CCR2^-$ (purple) and $Ly6C^+CCR2^+$ (blue). (D) Pie chart showing the distribution of FEMS shown in (C), n = 5. (E–F) CCR2 is critical for macrophage-associated fibrin endocytosis. Quantification of all FEMS (E), $Ly6C^+$ FEMS (F), and $Ly6C^-$ FEMS (G) in dermis of CCR2-deficient mice (*Ccr2* –/–) and CCR2-expressing littermates (*Ccr2* +/–) with implantation of fluorescent fibrin, n = 4–6. A two-tailed Student's *t*-test was used to test for significance (B and E–G).

knock-in mice in order to separate fibrin-endocytosing macrophages (FEMS) based on CCR2 expression as well as Ly6C expression, to distinguish recruited and dermal macrophages (Fig. 7C). Using these markers, four separate subtypes of FEMS were identified (Fig. 7C). By far the majority belonged to the $Ly6C^+CCR2^+$ inflammatory subtype, followed by the $Ly6C^-CCR2^+$ subtype (69%

and 22% of fibrin-positive macrophages, respectively, Fig. 7D). Because of the dominance of CCR2+ inflammatory macrophages in this process (a combined 91% of FEMS), we also assessed the role of CCR2-signaling in the recruitment of macrophages to the fibrin implantation site using *Ccr2* +/– and *Ccr2* –/– mice. In this experiment, we recorded a very large reduction in the number of FEMS in the CCR2-deficient mice (Fig. 7E), caused by a complete loss of $Ly6C^+$ macrophages (Fig. 7F), with little or no contribution from $Ly6C^-$ macrophages (Fig. 7G). In conclusion, $Ly6C^+CCR2^+$ inflammatory macrophages, recruited to the site of tissue injury in a CCR2-dependent process, constituted the main fibrin-endocytosing and -degrading cell type. Fibrin-endocytosis potential for each macrophage subpopulation is also listed in Table 1.

## Discussion

Macrophage-mediated ECM turnover is an integral part of tissue remodeling and tissue repair [38]. Using a novel flow cytometry-based assay, we here were able to provide high-resolution phenotyping of macrophage subtypes involved in endocytic matrix turnover in the dermis (Table 1 and Fig. 8). The assay allowed us to define specific properties and functional mechanisms for each subset of macrophages, including surface marker expression, mechanism of ECM endocytosis, status as recruited or resident macrophages, and cytokine signaling pathways regulating ECM-endocytic activity. Data obtained here were generally consistent with data obtained from previous microscopy-based studies, *i.e.*, we were able to solidify that macrophages are the most abundant collagen- and fibrin-endocytosing cells, that M2-like macrophages with a potent dextran-uptake potential contribute to the endocytosis of collagen in a MR-dependent process, and that CCR2-positive macrophages are the principal fibrin-endocytosing cells. However, several unexpected findings also emerged. Perhaps most surprising was the significant contribution of "inflammatory" macrophages (as defined by high CCR2 expression) not only to endocytic fibrin degradation, but also to endocytic collagen degradation, and the high dependence of collagen degradation on the integrity of the CCL2/MCP1-CCR2 signaling axis, which is typically associated with skewing macrophages towards an inflammatory rather than a wound healing phenotype. Thus, 67% of CEMS were CCR2-positive, and 79% of these could be classified as "resident inflammatory" macrophages (based on the absence of Ly6C expression), with the remaining 21% being classical Ly6C-positive and CCR2-positive "recruited inflammatory macrophages". The shared expression of surface markers clearly

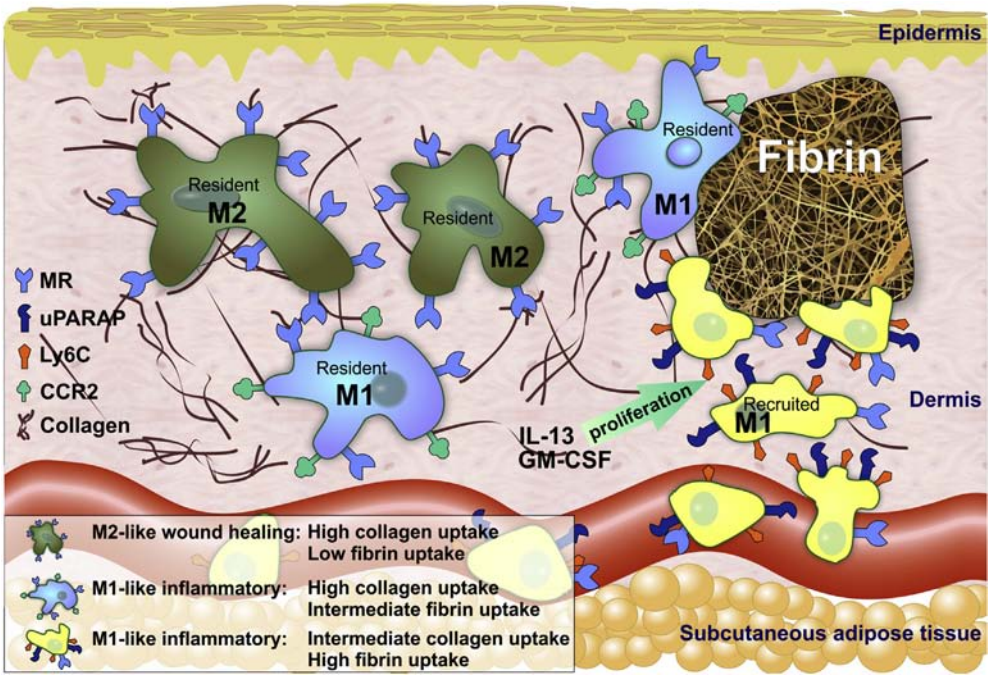


**Fig. 8.** Macrophage-mediated turnover of collagen and fibrin in dermis. ECM turnover in the remodeling dermis mediated by the three collagen- and fibrin-degrading macrophage subtypes identified in this study. For each macrophage subtype, the illustration summarizes: 1) Classification as inflammatory, M1-like or wound healing, M2-like macrophage. 2) Status as resident or recruited macrophage. 3) Expression of collagen receptors MR and uPARAP. 4) Expression of CCR2 and Ly6C. 5) Proposed mechanism of ECM turnover stimulation induced by the cytokines GM-CSF and IL-13.

**Table 2.** Primers used for genotyping mouse strains.

| Mouse strain | Primer names | Primer sequences | Annealing |
|---|---|---|---|
| C57BL6/Mrc1$^{tm1Mnz}$/J | MRmut_F | 5′-CAAGATCCGCCACAACATCG-3′ | 55 °C |
| | MRcommon_R | 5′-AGCCCTGATCTGTTCCTACG-3′ | |
| | MRwt_F | 5′-ATGAGGCTTCTCCTGCTTCT-3′ | 55 °C |
| | MRcommon_R | 5′-AGCCCTGATCTGTTCCTACG-3′ | |
| C57BL6/Mrc2$^{tm1Bug}$ | uPARAPmut_F | 5′-TCCTACAAATACACGCTGGCGATA-3′ | 60 °C |
| | uPARAPmut_R | 5′-GCAGTTCCCTTTTAAATGCAAATCA-3′ | |
| | uPARAPwt_F | 5′-TCTACACCATCCAGGGAAACTCAC-3′ | |
| | uPARAPwt_R | 5′-TTAAACTGGTAACAGCTGTCAGTC-3′ | |
| BALB/c-Il4ra$^{tm1Sz}$/J | IL4Ramut_F | 5′-CCAGACTGCCTTGGGAAAAG-3′ | 65 °C |
| | IL4Rawt_F | 5′-TGTGGGCTCAGAGTGACCAT-3′ | |
| | IL4Racommon_R | 5′-CAGGGAACAGCCCAGAAAAG-3′ | |
| C57BL6/Plg$^{tm1Jld}$/J | Plgcommon_F | 5′-TGTGGGCTCTAAAGATGGAACTCC-3′ | 65 °C |
| | Plgmut_R | 5′-GTGCGAGGCCAGAGGCCACTTGTGTAGCG-3′ | |
| | Plgwt_R | 5′-GACAAGGGGACTCGCTGGATGGCTA-3′ | |
| B6.129(Cg)-Ccr2$^{tm2.1Ifc}$/J | CCR2mut_R | 5′-CTTGATGACGTCCTCGGAG-3′ | 65 °C |
| | CCR2wt_R | 5′-GGAGTAGAGTGGAGGCAGGA-3′ | |
| | CCR2common_F | 5′-TAAACCTGGTCACCACATGC-3′ | |

suggests that Ly6C-positive, CCR2-positive CEMS derive from classical, circulating inflammatory macrophages [10]. The origin of the Ly6C-negative, CCR2-positive macrophages is less obvious. Based on our experiments demonstrating that genetic ablation of CCR2 substantially reduced the number of both Ly6C-negative and Ly6C-positive inflammatory macrophages endocytosing collagen, we speculate that these "resident inflammatory" macrophages are derived from Ly6C-positive and CCR2-positive monocytes that lose Ly6C expression subsequent to dermal residency. Indeed, local reprogramming-induced Ly6C loss has been previously reported for macrophages recruited to fibrotic lesions of the liver and was found to be associated with increased expression of ECM-degrading proteases [39]. The majority of the remaining CEMS were Ly6C-negative, expressed low levels of CCR2 and high levels of F4/80 and MR, and potently endocytosed dextran, all consistent with these cells being resident M2-like macrophages derived from a bone-marrow-independent myeloid cell population [35,40].

We previously found that MR is the dominant collagen endocytosis receptor utilized by macrophages, but we also reported a small contribution of uPARAP to macrophage-mediated collagen uptake [9]. The current study was able to resolve the utilization of the two receptors in terms of macrophage subtype, revealing a strong dependence of Ly6C-negative macrophages on MR for collagen uptake, and a relative independence of Ly6C-positive macrophages on MR for collagen uptake, with some contribution of uPARAP. It remains to be established whether MR-dependent, uPARAP-dependent, and MR- and uPARAP-independent collagen uptake is associated with differential macrophage functions or is involved in shaping macrophage phenotypes. In this regard, it should be noted that both receptors bind and endocytose other ligands besides collagen, including foreign and self-antigens for antigen presentation and collectins, and that collagen engagement may modulate these functions [41–49].

The CCR2/MCP1-CCL2 signaling axis is essential for appropriate tissue repair in models of skin wound healing and lung regeneration by promoting angiogenesis and proliferation of epithelial cells [50,51]. The current study suggests that this chemokine axis also promotes tissue repair through ECM remodeling. Likewise, the cytokine, GM-CSF, potently stimulated collagen endocytosis by specifically increasing the number of Ly6C-positive and CCR2-positive collagen-uptaking cells. This increase likely could be attributed to the local induction of proliferation of these dermal macrophages, as judged by the ability of GM-CSF to stimulate the proliferation of cultured macrophages reported here, and the ability to stimulate the proliferation of keratinocytes reported by others [52]. This recording of a pro-wound healing activity of GM-CSF may offer mechanistic insights related to the impaired wound healing observed in mice with abolished GM-CSF activity and the promising potential of GM-CSF as a reagent for promoting wound healing in patients with chronic wounds [26,53,54]. M-CSF is crucial for the initial differentiation and survival of macrophages [55], but our findings here indicate that this cytokine has limited potential for further modulation of macrophage phenotype in the context of ECM turnover. More surprising was the relative independence of endocytic collagen degradation on the IL-4/IL4Ra signaling axis. IL-4 is well-established as a key promotor of wound healing-associated processes and has a documented role of stimulating MR expression [30]. Nevertheless, IL-4 augmentation, through direct dermal administration of the recombinant cytokine, or elimination of IL-4 signaling, through genetic ablation of the principal IL-4 receptor, had only modest effects on collagen endocytosis and MR expression by any of the macrophage

subsets analyzed in this study. It is likely that IL-4/IL-4Ra signaling regulates other wound healing-related processes, such as collagen fibril assembly [56]. In contrast, the related cytokine, IL-13, markedly promoted endocytic collagen degradation, specifically through a large increase in the number of collagen-endocytosing Ly6C-positive and CCR2-positive recruited inflammatory macrophages. The latter observation is unexpected in light of the, at least partially shared, receptor subsets of IL-4 and IL-13 [57,58], and highlights the functional differences of the two wound healing-associated cytokines. It is also noteworthy that IL-13 stimulates collagen synthesis while at the same time stimulating macrophage-mediated collagen turnover [59,60].

In summary, we have shown that specific cytokine signaling pathways instruct phenotypically diverse subsets of macrophages to engage in endocytic ECM turnover in the context of dermal tissue remodeling. Future studies will reveal the degree to which the ECM-catabolic pathways identified here contribute to ECM remodeling in different physiological and pathological contexts.

## Methods

### Reagents and cells

The following reagents were purchased from commercial sources: Collagen type I from rat tail (BD Biosciences, Franklin Lakes, NJ), Tissue-Tek® Biopsy Cryomold® (10 mm × 10 mm × 5 mm, Sakura Finetek USA, Inc.), plasminogen-depleted, FXIII-containing fibrinogen from human plasma and citrate-free thrombin from human plasma (Merck Millipore, Darmstadt, Germany), AF647 labeling kit, AF488-conjugated 10 kDa dextran and AF647-conjugated human fibrinogen (Life Technologies, Grand Island, NY), Collagenase Type I, DNase Type I, and Neutral Protease (Worthington Biochemical, Lakewood, NJ), Rat-anti-Mouse MR/CD206 monoclonal antibody (clone MR5D3, Bio-Rad, Hercules, CA), Rabbit-anti-Rat secondary HRP-conjugated antibody (Dako, Glostrup, Denmark). Recombinant IL-4, IL-13, M-CSF, and GM-CSF (R&D systems, Minneapolis, MN). Monoclonal mouse anti-uPARAP antibody 2h9 was described previously [61]. Reagents and antibodies used for flow cytometry are described in the flow cytometry section below.

### Animal experiments, breeding and genotyping

Mice homozygous for a targeted mutation in the *Mrc1* gene (encoding MR) (C57BL6/Mrc1$^{tm1Mnz}$/J, RRID:MGI:3723178) [43], the *Mrc2* gene (encoding uPARAP) (C57BL6/Mrc2$^{tm1Bug}$, RRID:MGI:2677820) [21], the *IL4Ra* gene (encoding IL4Ra) [37] (RRID:MGI:3844327), and the *Plg* gene (encoding plasminogen) (C57BL6/Plg$^{tm1Jld}$/J, RRID:IMSR_JAX:002830) [62] and corresponding wild type littermate controls were generated by interbreeding mice heterozygous for each gene. Littermate mice heterozygous or homozygous for a targeted mutation in the *Ccr2* gene and knock-in of the RFP reporter gene (B6.129(Cg)-*Ccr2*$^{tm2.1Ifc}$/J, RRID:IMSR_JAX:017586) [13] were generated by interbreeding heterozygous (CCR2 +/–) mice or by breeding heterozygous mice with homozygous mice. Genotyping of offspring was performed using PCR with the primers and annealing temperatures listed in Table 2. Female mice with an age of 7–9 weeks were used in all experiments, except for the *Plg* strain for which males of the same age were also included. The total number of animals included in this study was 144, distributed as follows: collagen injection, 110; fibrin implantation, 22; harvest of bone marrow cells for generation of macrophages 12. All experiments involving mice were performed in an Association for Assessment and Accreditation of Laboratory Animals Care International–accredited vivarium following institutional guidelines and standard operating procedures under approved animal study proposals.

### Fluorescent labeling of collagen

Fluorescent labeling of collagen type I was performed as described previously [9]. Acid-extracted rat tail collagen (BD Biosciences) in 13 mM HCl was neutralized and brought to a final concentration of 0.5 mg/mL collagen in a volume of 5 mL using phosphate-buffered saline (PBS). The collagen was then allowed to polymerize into a gel by incubation at 37 °C for 2 h. The resultant gel was washed in sterile water and subsequently incubated with 100 µg amino-reactive AF647 succinimidyl ester (Life Technologies) in a 0.1 M $NaHCO_3$ buffer for 2 h. After the labeling reaction, the AF647 collagen gels were washed extensively in sterile PBS for 2–3 days at room temperature to remove excess dye and collagen incapable of forming fibrils while in a labeled state. The labeled collagen was then re-solubilized using 13 mM HCl and stored at 4 °C. Non-solubilized collagen was removed by centrifugation for 60 min at 45,000*g*.

### *In vivo* assay for collagen uptake in dermis

Mice were anesthetized using isoflurane and shaved on the back and both flanks. AF647-labeled collagen was mixed with AF488-labeled 10 kDa dextran and neutralized with PBS containing 50 mM HEPES. Final concentrations in the neutralized solution were 200 µg/mL AF647-collagen and 40 µg/mL AF488-dextran. Immediately after neutralization, the mixture was injected subcutaneously at

three separates sites on the back and flanks of each mouse (60 µL per injection site). 24 h later, an approximate 2.5 × 2.5 cm piece of skin covering all three injections sites was removed and dermal cells isolated for flow cytometry as described below. In experiments in which the effect of cytokines on collagen internalization and degradation were examined, 1 µg of recombinant mouse M-CSF, GM-CSF, IL-4 or IL-13 was included in each 60 µL injection of collagen and dextran.

### Formation and implantation of fluorescent fibrin gels

The formation of fluorescent polymerized fibrin gels from human fibrinogen was performed according to a previously developed procedure [8]. In brief, plasminogen-depleted, Factor XIII-containing fibrinogen from human plasma was dissolved in Dulbecco Modified Eagle Medium (DMEM) to a concentration of 10 mg/mL at 37 °C. To 245 µL of unlabeled fibrinogen, 5 µL of 5 mg/mL AF647-conjugated human fibrinogen was then added to yield a fibrinogen mixture containing approximately 1% fluorescent fibrinogen. To form a polymerized fluorescent fibrin gel, 250 µL of the fibrinogen solution was then mixed quickly with 250 µL DMEM containing 6 U/mL of thrombin in a 10 mm × 10 mm × 5 mm Tissue-Tek® Biopsy Cryomold® (Sakura Finetek), which was then sealed with a cover glass. The polymerization reaction was then performed at 37 °C for 3–4 h. The resulting fibrin gels were washed twice in 25 mL of sterile PBS for 15 min and then once overnight. All incubations and washes were performed in the dark to minimize exposure of fluorescent fibrin to light. To implant the fibrin gels, mice were anesthetized using isoflurane and shaved on the back and both flanks. Using aseptic techniques, a 1 cm dorsal incision was made on the left side of the spine and the fibrin gels placed into a subcutaneous pocket made on the right side of the spine. The incision was then closed using wound clips. 24 h later, an approximate 2.5 × 2.5 cm piece of skin covering the implanted fibrin, but not including the site of the incision, was removed and dermal cells isolated for flow cytometry as described below.

### Flow cytometry

Skin tissue excised for flow cytometry was immediately placed on ice and washed once with 1 mL of ice cold DMEM. Next, fine scissors were used to cut the skin samples into small pieces, which were then placed in a digestion mixture consisting of DMEM supplemented with 2.1 mg/mL Collagenase Type I, 75 µg/mL Deoxyribonuclease Type I, 0.125 mg/mL Neutral Protease (Worthington Biochemical) and 5 mM $CaCl_2$ and incubated with gentle shaking at 4 °C overnight followed by 1 h at 37 °C. 10 mL of ice cold DMEM was then added to the digested skin, followed by filtering through a 70 µm mesh to remove remaining tissue fragments from liberated cells in suspension. Filtered cell suspensions were then centrifuged at 300*g* for 5 min, washed once in PBS, and stained at room temperature for 15 min with a 1:200 dilution of Zombie Violet Live/Dead stain in PBS (Biolegend, San Diego, California). Cells were washed in ice cold staining buffer (PBS supplemented with 1% BSA) and kept on ice for the remainder of the procedure. Before antibody staining, FC-receptors were blocked for at least 15 min using a 1:10 dilution of mouse FC-blocking reagent (Miltenyi Biotec, Auburn, California). Cells were then stained with one of the following sets of antibodies. Set 1 (used for staining cells from CCR2.RFP transgenic mice): Anti-CD45 (Clone 30-F11, AF700, Biolegend, 1:100 dilution), anti-F4/80 (Clone BM8, BV785, Biolegend, 1:100), anti-Ly6C (Clone HK1.4, PE-Cy7, Biolegend, 1:2500), anti-MR (Clone C068C2, BV605, Biolegend, 1:50); set 2: Anti-CD45 (Clone 30-F11, BV605, Biolegend, 1:100 dilution), anti-F4/80 (Clone BM8, BV785, Biolegend, 1:100), anti-Ly6C (Clone HK1.4, PE-Cy7, Biolegend, 1:2500), and either anti-CD11b (Clone M1/70, PE, Biolegend, 1:200), anti-IL4Ra (Clone mIL4R-M1, PE, BD Biosciences, 1:50) or anti-GM-CSFR (clone 698423, PE, R&D systems, 1:50). Antibody stains were performed in staining buffer for 1 h. Stained cells were washed twice in staining buffer and filtered through a 40 µm mesh. Flow analysis for surface marker expression, RFP expression, Zombie Violet Live/Dead stain, uptake of AF647-labeled collagen, AF488-labeled 10 kDa dextran or AF647-labeled fibrin was performed using a Fortessa II instrument (BD Biosciences). Positive and negative gates for each surface marker or for cells positive for fluorescent ligand uptake was set using fluorescence minus one (FMO) controls, in which each fluorophore in turn was excluded.

### Generation of primary macrophages from bone marrow cells

Pelvis, femur, and tibia were excised from MR- and uPARAP-deficient mice and their corresponding wild type littermates immediately after euthanasia. The excised bones were placed on wet ice in a PBS buffer containing 3% fetal calf serum (FCS) after removal of soft tissue using scissors and paper towels. The bones from each mouse were crushed using mortars and rinsed extensively in Roswell Park Memorial Institute (RPMI)-1640 medium containing 10% FCS and 1% penicillin/streptomycin in order to liberate the marrow cells and bring them into suspension. Bone marrow cell suspensions were then filtered through a 40 µm mesh to remove remaining pieces of tissue. Red blood cells were removed next using a Red Blood Cell lysis buffer according to the manufacturer's instructions

(Biolegend). Bone marrow cells were seeded at a density of 1–1.25 × $10^6$ cells/mL in RPMI-1640 containing 10% FCS, 1% penicillin/streptomycin (growth medium) and either 20 ng/mL M-CSF or GM-CSF or with no cytokines added. For the assessment of cell proliferation, a total of 5 × $10^6$ cells were seeded in culture flasks. The total number of cells in suspension and adhering to the surface was then recorded after 4 days. For Western blot analysis of collagen receptor expression, 5 × $10^6$ cells were seeded in culture flasks in growth medium containing 20 ng/mL M-CSF or GM-CSF. After 4 days, the medium was removed and fresh growth medium containing 20 ng/mL M-CSF or GM-CSF alone or in combination with 20 ng/mL IL-4, 10 ng/mL IL-13 or both, was added. At day 6, cells were harvested, washed 3 times in PBS and lysed using a 1% Triton X-100 lysis buffer containing Protease Inhibitor Cocktail III (1:200, Sigma). Western blotting for MR and uPARAP was performed as described below. To assay for the internalization of fluorescent collagen, 1.5 × $10^6$ cells were seeded in 12-well culture plates in growth medium containing 20 ng/mL M-CSF. At day 4, fresh growth medium containing 20 ng/mL M-CSF alone or in combination with 20 ng/mL IL-4 or 10 ng/mL IL-13 was added. At day 6, AF647-labeled collagen was added to each well in a final concentration of 13 μg/mL. The internalization experiment was terminated by removing the medium and washing the cells 3 times in ice cold PBS. Cells were then incubated in an ice-cold trypsin/EDTA solution for 10 min and removed from the surface of the culture plates using cell scrapers. Trypsin/EDTA was removed by centrifugation of cells at 300*g* for 5 min and washing in 1 mL of PBS containing 3% fetal calf serum. Collagen internalization was then quantified by analyzing the cells using a LSR-II flow cytometer (BD Biosciences).

### Western blotting

Protein concentrations in cell lysates from bone marrow-derived macrophages were first determined using a BCA protein concentration kit (Bio-Rad). For the analysis of uPARAP and MR expression, 12 μg of protein from each lysate was separated by SDS-PAGE and blotted onto a PVDF membrane. 2% BSA solution was used for blocking. Primary mouse anti-uPARAP mAb 2h9 (0.5 μg/mL) [61] or rat anti-MR (1 μg/mL, clone MR5D3, Bio-Rad) diluted in a 0.1% Tween20 PBS solution were applied overnight at 4 °C. Secondary Rabbit-anti-mouse or Rabbit-anti-Rat HRP conjugated antibodies (Dako) were applied at a 1:3000 dilution in 0.1% Tween20 PBS solution. ECL western blotting detection reagents and High Performance Chemiluminescence films (GE Healthcare) were used for development. For loading controls, 10 μg of protein from each lysate was separated by SDS-PAGE and stained with Coomassie brilliant blue to visualize proteins in each lysate.

### Statistics

All statistical analyses were performed using GraphPad Prism version 7 for Mac software. A two-tailed Student's *t*-test was used to test for significance when comparing two experimental groups. For comparisons including more than two experimental groups, a one-way ANOVA was used. A p-value of less than 0.05 was considered significant for all statistical tests.

Supplementary data to this article can be found online at https://doi.org/10.1016/j.mbplus.2019.03.002.

## Acknowledgments

This work was supported by the NIDCR, NIH Intramural Research Program (THB), the NIDCR Veterinary Resources Core (Z number DE000740-05) and Combined Technical core (ZIC DE000729-09), the Danish Medical Research Council/Danish Council for Independent Research (HJJ and NB), the Danish Cancer Society (HJJ, DHM and NB), Region Hovedstadens Forskningsfond (DHM and NB), the Novo Nordisk Foundation (DHM and NB), the European Commission (DHM), the Lundbeck Foundation and the Danish Cancer Research Foundation.

## Author contributions

Henrik J. Jürgensen: Conceptualization; data curation; formal analysis; funding acquisition; investigation; methodology; visualization; roles/writing - original draft; writing - review & editing. Lakmali M. Silva: Investigation; writing - review & editing. Oliver Krigslund: Investigation; writing - review & editing. Sander van Putten: Investigation; writing - review & editing. Daniel H. Madsen: Methodology; supervision; writing - review & editing. Niels Behrendt: Resources; supervision; writing - review & editing. Lars H. Engelholm: Resources; supervision; visualization; writing - review & editing. Thomas H. Bugge: Formal analysis; project administration; resources; methodology; supervision; conceptualization; roles/writing - original draft; writing - review & editing.

*Received 23 January 2019;*
*Received in revised form 11 March 2019;*
*Accepted 12 March 2019*
Available online 19 March 2019

***Keywords:***
Collagen degradation;
Extracellular matrix endocytosis;
Fibrin degradation;

Mannose receptor/CD206;
uPARAP/Endo180

***Abbreviations used:***

AF, Alexa Fluor; CEMS, collagen-endocytosing macrophages; CCL2/MCP-1, chemokine (C-C motif) ligand 2/monocyte chemoattractant protein 1; CCR2, C-C chemokine receptor type 2; ECM, extracellular matrix; FEMS, fibrin-endocytosing macrophages; FMO, fluorescence minus one; GM-CSF, Granulocyte Macrophage-Colony Stimulating Factor; GM-CSFR, GM-CSF Receptor; IL, Interleukin; IL4Ra, IL4 Receptor a; M-CSF, Macrophage-Colony Stimulating Factor; MR, mannose receptor/CD206; Plg, plasminogen; RFP, red fluorescent protein; uPARAP, urokinase plasminogen activator receptor associated protein/Endo180.

## References


[1] S.S. Apte, W.C. Parks, Metalloproteinases: a parade of functions in matrix biology and an outlook for the future, Matrix Biol. 44-46 (2015) 1–6.

[2] C. Bonnans, J. Chou, Z. Werb, Remodelling the extracellular matrix in development and disease, Nat Rev Mol Cell Biol 15 (2014) 786–801.

[3] M.A. Petersen, J.K. Ryu, K. Akassoglou, Fibrinogen in neurological diseases: mechanisms, imaging and therapeutics, Nat. Rev. Neurosci. 19 (2018) 283–301.

[4] M.M. Mohamed, B.F. Sloane, Cysteine cathepsins: multifunctional enzymes in cancer, Nat. Rev. Cancer 6 (2006) 764–775.

[5] Linsenmayer, T. F. (1991) Collagen, Plenum Press.

[6] M. van der Rest, R. Garrone, Collagen family of proteins, FASEB J. 5 (1991) 2814–2823.

[7] R.F. Doolittle, Fibrinogen and fibrin, Annu. Rev. Biochem. 53 (1984) 195–229.

[8] M.P. Motley, D.H. Madsen, H.J. Jurgensen, D.E. Spencer, R. Szabo, K. Holmbeck, M.J. Flick, D.A. Lawrence, F.J. Castellino, R. Weigert, T.H. Bugge, A CCR2 macrophage endocytic pathway mediates extravascular fibrin clearance in vivo, Blood 127 (2016) 1085–1096.

[9] D.H. Madsen, D. Leonard, A. Masedunskas, A. Moyer, H.J. Jurgensen, D.E. Peters, P. Amornphimoltham, A. Selvaraj, S. S. Yamada, D.A. Brenner, S. Burgdorf, L.H. Engelholm, N. Behrendt, K. Holmbeck, R. Weigert, T.H. Bugge, M2-like macrophages are responsible for collagen degradation through a mannose receptor-mediated pathway, J. Cell Biol. 202 (2013) 951–966.

[10] F. Geissmann, S. Jung, D.R. Littman, Blood monocytes consist of two principal subsets with distinct migratory properties, Immunity 19 (2003) 71–82.

[11] T.B. Thornley, Z. Fang, S. Balasubramanian, R.A. Larocca, W. Gong, S. Gupta, E. Csizmadia, N. Degauque, B.S. Kim, M. Koulmanda, V.K. Kuchroo, T.B. Strom, Fragile TIM-4-expressing tissue resident macrophages are migratory and immunoregulatory, J. Clin. Invest. 124 (2014) 3443–3454.

[12] C. Shi, E.G. Pamer, Monocyte recruitment during infection and inflammation, Nat Rev Immunol 11 (2011) 762–774.

[13] N. Saederup, A.E. Cardona, K. Croft, M. Mizutani, A.C. Cotleur, C.L. Tsou, R.M. Ransohoff, I.F. Charo, Selective chemokine receptor usage by central nervous system myeloid cells in CCR2-red fluorescent protein knock-in mice, PLoS One 5 (2010), e13693.

[14] D.M. Mosser, J.P. Edwards, Exploring the full spectrum of macrophage activation, Nat Rev Immunol 8 (2008) 958–969.

[15] R.M. Sandoval, M.D. Kennedy, P.S. Low, B.A. Molitoris, Uptake and trafficking of fluorescent conjugates of folic acid in intact kidney determined using intravital two-photon microscopy, Am J Physiol Cell Physiol 287 (2004) C517–C526.

[16] A. Masedunskas, R. Weigert, Intravital two-photon microscopy for studying the uptake and trafficking of fluorescently conjugated molecules in live rodents, Traffic 9 (2008) 1801–1810.

[17] L. Martinez-Pomares, D. Wienke, R. Stillion, E.J. McKenzie, J.N. Arnold, J. Harris, E. McGreal, R.B. Sim, C.M. Isacke, S. Gordon, Carbohydrate-independent recognition of collagens by the macrophage mannose receptor, Eur. J. Immunol. 36 (2006) 1074–1082.

[18] D.H. Madsen, S. Ingvarsen, H.J. Jurgensen, M.C. Melander, L. Kjoller, A. Moyer, C. Honore, C.A. Madsen, P. Garred, S. Burgdorf, T.H. Bugge, N. Behrendt, L.H. Engelholm, The non-phagocytic route of collagen uptake: a distinct degradation pathway, J. Biol. Chem. 286 (2012) 26996–27010.

[19] D.H. Madsen, H.J. Jurgensen, M.S. Siersbaek, D.E. Kuczek, L. Grey Cloud, S. Liu, N. Behrendt, L. Grontved, R. Weigert, T.H. Bugge, Tumor-associated macrophages derived from circulating inflammatory monocytes degrade collagen through cellular uptake, Cell Rep. 21 (2017) 3662–3671.

[20] A. Wollenberg, M. Mommaas, T. Oppel, E.M. Schottdorf, S. Gunther, M. Moderer, Expression and function of the mannose receptor CD206 on epidermal dendritic cells in inflammatory skin diseases, J Invest Dermatol 118 (2002) 327–334.

[21] L.H. Engelholm, K. List, S. Netzel-Arnett, E. Cukierman, D.J. Mitola, H. Aaronson, L. Kjoller, J.K. Larsen, K.M. Yamada, D. K. Strickland, K. Holmbeck, K. Dano, H. Birkedal-Hansen, N. Behrendt, T.H. Bugge, uPARAP/Endo180 is essential for cellular uptake of collagen and promotes fibroblast collagen adhesion, J. Cell Biol. 160 (2003) 1009–1015.

[22] D. Wienke, J.R. MacFadyen, C.M. Isacke, Identification and characterization of the endocytic transmembrane glycoprotein Endo180 as a novel collagen receptor, Mol. Biol. Cell 14 (2003) 3592–3604.

[23] L. East, A. McCarthy, D. Wienke, J. Sturge, A. Ashworth, C. M. Isacke, A targeted deletion in the endocytic receptor gene Endo180 results in a defect in collagen uptake, EMBO Rep. 4 (2003) 710–716.

[24] A.L. Croxford, M. Lanzinger, F.J. Hartmann, B. Schreiner, F. Mair, P. Pelczar, B.E. Clausen, S. Jung, M. Greter, B. Becher, The cytokine GM-CSF drives the inflammatory signature of CCR2+ monocytes and licenses autoimmunity, Immunity 43 (2015) 502–514.

[25] A. Francisco-Cruz, M. Aguilar-Santelises, O. Ramos-Espinosa, D. Mata-Espinosa, B. Marquina-Castillo, J. Barrios-Payan, R. Hernandez-Pando, Granulocyte-macrophage colony-stimulating factor: not just another haematopoietic growth factor, Med. Oncol. 31 (2014), 774.

[26] S. Barrientos, O. Stojadinovic, M.S. Golinko, H. Brem, M. Tomic-Canic, Growth factors and cytokines in wound healing, Wound Repair Regen. 16 (2008) 585–601.

[27] K. Klinkert, D. Whelan, A.J.P. Clover, A.L. Leblond, A.H.S. Kumar, N.M. Caplice, Selective M2 macrophage depletion leads to prolonged inflammation in surgical wounds, Eur. Surg. Res. 58 (2017) 109–120.

[28] K.P. MacDonald, J.S. Palmer, S. Cronau, E. Seppanen, S. Olver, N.C. Raffelt, R. Kuns, A.R. Pettit, A. Clouston, B. Wainwright, D. Branstetter, J. Smith, R.J. Paxton, D.P. Cerretti, L. Bonham, G.R. Hill, D.A. Hume, An antibody against the colony-stimulating factor 1 receptor depletes the resident subset of monocytes and tissue- and tumor-associated macrophages but does not inhibit inflammation, Blood 116 (2010) 3955–3963.

[29] P. Loke, M.G. Nair, J. Parkinson, D. Guiliano, M. Blaxter, J.E. Allen, IL-4 dependent alternatively-activated macrophages have a distinctive in vivo gene expression phenotype, BMC Immunol. 3 (2002) 7.

[30] M. Stein, S. Keshav, N. Harris, S. Gordon, Interleukin 4 potently enhances murine macrophage mannose receptor activity: a marker of alternative immunologic macrophage activation, J. Exp. Med. 176 (1992) 287–292.

[31] A.G. Doyle, G. Herbein, L.J. Montaner, A.J. Minty, D. Caput, P. Ferrara, S. Gordon, Interleukin-13 alters the activation state of murine macrophages in vitro: comparison with interleukin-4 and interferon-gamma, Eur. J. Immunol. 24 (1994) 1441–1445.

[32] S.J. Van Dyken, R.M. Locksley, Interleukin-4- and interleukin-13-mediated alternatively activated macrophages: roles in homeostasis and disease, Annu. Rev. Immunol. 31 (2013) 317–343.

[33] J.A. Knipper, S. Willenborg, J. Brinckmann, W. Bloch, T. Maass, R. Wagener, T. Krieg, T. Sutherland, A. Munitz, M.E. Rothenberg, A. Niehoff, R. Richardson, M. Hammerschmidt, J.E. Allen, S.A. Eming, Interleukin-4 receptor alpha signaling in myeloid cells controls collagen fibril assembly in skin repair, Immunity 43 (2015) 803–816.

[34] A.E. Postlethwaite, M.A. Holness, H. Katai, R. Raghow, Human fibroblasts synthesize elevated levels of extracellular matrix proteins in response to interleukin 4, J. Clin. Invest. 90 (1992) 1479–1485.

[35] S.J. Jenkins, D. Ruckerl, P.C. Cook, L.H. Jones, F.D. Finkelman, N. van Rooijen, A.S. MacDonald, J.E. Allen, Local macrophage proliferation, rather than recruitment from the blood, is a signature of TH2 inflammation, Science 332 (2011) 1284–1288.

[36] X. Liao, N. Sharma, F. Kapadia, G. Zhou, Y. Lu, H. Hong, K. Paruchuri, G.H. Mahabeleshwar, E. Dalmas, N. Venteclef, C. A. Flask, J. Kim, B.W. Doreian, K.Q. Lu, K.H. Kaestner, A. Hamik, K. Clement, M.K. Jain, Kruppel-like factor 4 regulates macrophage polarization, J. Clin. Invest. 121 (2011) 2736–2749.

[37] N. Noben-Trauth, L.D. Shultz, F. Brombacher, J.F. Urban Jr., H. Gu, W.E. Paul, An interleukin 4 (IL-4)-independent pathway for CD4+ T cell IL-4 production is revealed in IL-4 receptor-deficient mice, Proc. Natl. Acad. Sci. U. S. A. 94 (1997) 10838–10843.

[38] K.S. Smigiel, W.C. Parks, Macrophages, wound healing, and fibrosis: recent insights, Curr. Rheumatol. Rep. 20 (2018) 17.

[39] P. Ramachandran, A. Pellicoro, M.A. Vernon, L. Boulter, R.L. Aucott, A. Ali, S.N. Hartland, V.K. Snowdon, A. Cappon, T.T. Gordon-Walker, M.J. Williams, D.R. Dunbar, J.R. Manning, N. van Rooijen, J.A. Fallowfield, S.J. Forbes, J.P. Iredale, Differential Ly-6C expression identifies the recruited macrophage phenotype, which orchestrates the regression of murine liver fibrosis, Proc. Natl. Acad. Sci. U. S. A. 109 (2012) E3186–E3195.

[40] C. Schulz, E. Gomez Perdiguero, L. Chorro, H. Szabo-Rogers, N. Cagnard, K. Kierdorf, M. Prinz, B. Wu, S.E. Jacobsen, J.W. Pollard, J. Frampton, K.J. Liu, F. Geissmann, A lineage of myeloid cells independent of Myb and hematopoietic stem cells, Science 336 (2012) 86–90.

[41] R.A. Ezekowitz, D.J. Williams, H. Koziel, M.Y. Armstrong, A. Warner, F.F. Richards, R.M. Rose, Uptake of Pneumocystis carinii mediated by the macrophage mannose receptor, Nature 351 (1991) 155–158.

[42] H. Irjala, E.L. Johansson, R. Grenman, K. Alanen, M. Salmi, S. Jalkanen, Mannose receptor is a novel ligand for L-selectin and mediates lymphocyte binding to lymphatic endothelium, J. Exp. Med. 194 (2001) 1033–1042.

[43] S.J. Lee, S. Evers, D. Roeder, A.F. Parlow, J. Risteli, L. Risteli, Y.C. Lee, T. Feizi, H. Langen, M.C. Nussenzweig, Mannose receptor-mediated regulation of serum glycoprotein homeostasis, Science 295 (2002) 1898–1901.

[44] L. Martinez-Pomares, P.R. Crocker, R. Da Silva, N. Holmes, C. Colominas, P. Rudd, R. Dwek, S. Gordon, Cell-specific glycoforms of sialoadhesin and CD45 are counter-receptors for the cysteine-rich domain of the mannose receptor, J. Biol. Chem. 274 (1999) 35211–35218.

[45] R.A. Paveley, S.A. Aynsley, J.D. Turner, C.D. Bourke, S.J. Jenkins, P.C. Cook, L. Martinez-Pomares, A.P. Mountford, The Mannose Receptor (CD206) is an important pattern recognition receptor (PRR) in the detection of the infective stage of the helminth Schistosoma mansoni and modulates IFNgamma production, Int. J. Parasitol. 41 (2011) 1335–1345.

[46] T.I. Prigozy, P.A. Sieling, D. Clemens, P.L. Stewart, S.M. Behar, S.A. Porcelli, M.B. Brenner, R.L. Modlin, M. Kronenberg, The mannose receptor delivers lipoglycan antigens to endosomes for presentation to T cells by CD1b molecules, Immunity 6 (1997) 187–197.

[47] M.C. Tan, A.M. Mommaas, J.W. Drijfhout, R. Jordens, J.J. Onderwater, D. Verwoerd, A.A. Mulder, A.N. van der Heiden, T.H. Ottenhoff, M. Cella, A. Tulp, J.J. Neefjes, F. Koning, Mannose receptor mediated uptake of antigens strongly enhances HLA-class II restricted antigen presentation by cultured dendritic cells, Adv. Exp. Med. Biol. 417 (1997) 171–174.

[48] H.J. Jurgensen, K.S. Norregaard, M.M. Sibree, E. Santoni-Rugiu, D.H. Madsen, K. Wassilew, D. Krustrup, P. Garred, T. H. Bugge, L.H. Engelholm, N. Behrendt, Immune regulation by fibroblasts in tissue injury depends on uPARAP-mediated uptake of collectins, J. Cell Biol. 218 (2019) 333–349.

[49] S. Burgdorf, V. Schuette, V. Semmling, K. Hochheiser, V. Lukacs-Kornek, P.A. Knolle, C. Kurts, Steady-state cross-presentation of OVA is mannose receptor-dependent but inhibitable by collagen fragments, Proc. Natl. Acad. Sci. U. S. A. 107 (2010) E48–E49 (author reply E50-41).

[50] A.J. Lechner, I.H. Driver, J. Lee, C.M. Conroy, A. Nagle, R.M. Locksley, J.R. Rock, Recruited monocytes and type 2 immunity promote lung regeneration following pneumonectomy, Cell Stem Cell 21 (120–134) (2017), e127.

[51] S. Willenborg, T. Lucas, G. van Loo, J.A. Knipper, T. Krieg, I. Haase, B. Brachvogel, M. Hammerschmidt, A. Nagy, N. Ferrara, M. Pasparakis, S.A. Eming, CCR2 recruits an inflammatory macrophage subpopulation critical for angiogenesis in tissue repair, Blood 120 (2012) 613–625.

[52] A. Mann, K. Breuhahn, P. Schirmacher, M. Blessing, Keratinocyte-derived granulocyte-macrophage colony stimulating factor accelerates wound healing: stimulation of keratinocyte proliferation, granulation tissue formation, and vascularization, J Invest Dermatol 117 (2001) 1382–1390.

[53] Y. Fang, S.J. Gong, Y.H. Xu, B.D. Hambly, S. Bao, Impaired cutaneous wound healing in granulocyte/macrophage

colony-stimulating factor knockout mice, Br. J. Dermatol. 157 (2007) 458–465.
[54] A. Mann, K. Niekisch, P. Schirmacher, M. Blessing, Granulocyte-macrophage colony-stimulating factor is essential for normal wound healing, J Investig Dermatol Symp Proc 11 (2006) 87–92.
[55] I. Ushach, A. Zlotnik, Biological role of granulocyte macrophage colony-stimulating factor (GM-CSF) and macrophage colony-stimulating factor (M-CSF) on cells of the myeloid lineage, J. Leukoc. Biol. 100 (2016) 481–489.
[56] S. Knippen, T. Loning, V. Muller, C. Schroder, F. Janicke, K. Milde-Langosch, Expression and prognostic value of activating transcription factor 2 (ATF2) and its phosphorylated form in mammary carcinomas, Anticancer Res. 29 (2009) 183–189.
[57] K. Nelms, A.D. Keegan, J. Zamorano, J.J. Ryan, W.E. Paul, The IL-4 receptor: signaling mechanisms and biologic functions, Annu. Rev. Immunol. 17 (1999) 701–738.
[58] S. Fichtner-Feigl, W. Strober, K. Kawakami, R.K. Puri, A. Kitani, IL-13 signaling through the IL-13alpha2 receptor is involved in induction of TGF-beta1 production and fibrosis, Nat. Med. 12 (2006) 99–106.
[59] J.E. Kolodsick, G.B. Toews, C. Jakubzick, C. Hogaboam, T. A. Moore, A. McKenzie, C.A. Wilke, C.J. Chrisman, B.B. Moore, Protection from fluorescein isothiocyanate-induced fibrosis in IL-13-deficient, but not IL-4-deficient, mice results from impaired collagen synthesis by fibroblasts, J. Immunol. 172 (2004) 4068–4076.
[60] M. Jinnin, H. Ihn, K. Yamane, K. Tamaki, Interleukin-13 stimulates the transcription of the human alpha2(I) collagen gene in human dermal fibroblasts, J. Biol. Chem. 279 (2004) 41783–41791.
[61] J. Sulek, R.A. Wagenaar-Miller, J. Shireman, A. Molinolo, D. H. Madsen, L.H. Engelholm, N. Behrendt, T.H. Bugge, Increased expression of the collagen internalization receptor uPARAP/Endo180 in the stroma of head and neck cancer, J. Histochem. Cytochem. 55 (2007) 347–353.
[62] T.H. Bugge, M.J. Flick, C.C. Daugherty, J.L. Degen, Plasminogen deficiency causes severe thrombosis but is compatible with development and reproduction, Genes Dev. 9 (1995) 794–807.